CR137768

HAMILTON STANDARD Division of UNITED TECHNOLOGIES

SVHSER6784

DESIGN, DEVELOPMENT, AND FABRICATION OF A PROTOTYPE ICE PACK HEAT SINK SUBSYSTEM

FLIGHT EXPERIMENT PHYSICAL PHENOMENA EXPERIMENT CHEST

FINAL REPORT

BY

GEORGE J. ROEBELEN, JR
AND
W. CLARK DEAN, II

PREPARED UNDER CONTRACT NO. NAS 2-8665
BY
HAMILTON STANDARD
DIVISION OF UNITED TECHNOLOGIES CORPORATION
WINDSOR LOCKS, CONNECTICUT

FOR

NATIONAL AERONAUTICS AND SPACE ADMINISTRATION
AMES RESEARCH CENTER
MOFFETT FIELD, CALIFORNIA 94035

DECEMBER 1975

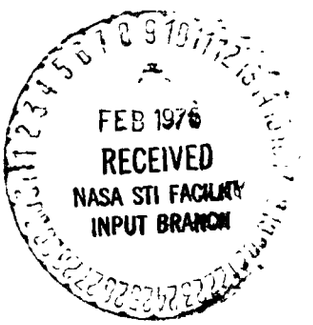

CR137768

SVHSER6784

HAMILTON STANDARD Division of UNITED TECHNOLOGIES

ABSTRACT

DESIGN, DEVELOPMENT, AND FABRICATION OF A PROTOTYPE
ICE PACK HEAT SINK SUBSYSTEM

FLIGHT EXPERIMENT PHYSICAL PHENOMENA EXPERIMENT CHEST

BY

GEORGE J. ROEBELEN, JR
AND
W. CLARK DEAN, II

CONTRACT NO. NAS 2-8665

This report describes the concepting of a Flight Experiment Physical Phenomena Experiment Chest to be used eventually for investigating and demonstrating Ice Pack Heat Sink Subsystem physical phenomena during a zero gravity flight experiment.

FOREWORD

This report has been prepared by the Hamilton Standard Division of United Technologies Corporation for the National Aeronautics and Space Administration Ames Research Center in accordance with the requirements of Contract NAS 2-8665, Design, Development, and Fabrication of a Prototype Ice Pack Heat Sink Subsystem - Flight Experiment Physical Phenomena Experiment Chest.

Appreciation is expressed to the NASA Technical Manager, Mr. James Blackaby of the Ames Research Center, for his guidance and advice.

Hamilton Standard personnel responsible for the conduct of this program were Mr. Fred H. Greenwood and Mr. Daniel J. Lizdas, Project Managers, Mr. George J. Roebelen, Jr, Program Engineer, and Mr. W. Clark Dean, II, Design Engineer. Appreciation is expressed to Mr. John S. Lovell, Chief, Advanced Engineering, Mr. Earl K. Moore, Technical Specialist, and Dr. John R. Aylward, Research Scientist, whose efforts made the successful completion of this program possible.

Detailed Flight Experiment Physical Phenomena Experiment Chest drawings have been prepared as a result of effort expended during the period covered by this report. These drawings, Physical Phenomena Experiment Chest-Schematic, SVSK 91539 sheet 1 and sheet 2, and Physcial Phenomena Experiment Chest-Hardware Arrangement, SVSK 91585 sheets 1, 2, 3, and 4 have been transmitted under separate cover.

TABLE OF CONTENTS

TABLE OF CONTENTS (CONT.)

TABLE OF CONTENTS (CONT.)

LIST OF FIGURES

LIST OF FIGURES (CONT.)

LIST OF TABLES

INTRODUCTION

Future manned space exploration missions are expected to include requirements for astronaut life support equipment capable of repeated use and regeneration for many extravehicular activity (EVA) sorties. In anticipation of these requirements, NASA ARC funded two contracts (NAS 2-6021 and NAS 2-6022) for the study of Advanced Extravehicular Protective Systems (AEPS). The purpose of these studies was to determine the most practical and promising concepts for manned space flight operations projected for the late 1970's and 1980's, and to identify areas where concentrated research would be most effective in the development of these concepts.

One regenerative concept for astronaut cooling utilizes an ice pack as the primary heat sink for a liquid cooled garment (LCG) cooling system. In an emergency, or for extended operations, water from the melted ice pack could be evaporated directly to space or supplied to an evaporative-type LCG heat exchanger. NASA ARC funded a contract (NAS 2-7011) which resulted in the design, fabrication, and test at one gravity of a prototype Ice Pack Heat Sink Subsystem; a study to uncover a material with a greater heat of fusion that could be substituted for water/ice as the thermal sink thereby reducing system weight and volume; and a plan for development of a candidate Shuttle/Spacelab flight experiment capable of demonstrating the performance of an Ice Pack Heat Sink Subsystem for astronaut cooling in zero gravity as well as providing data on the physical phenomena associated primarily with the heat transfer aspects of the operation of such a system. A portion of the Ice Pack Heat Sink Subsystem Flight Experiment Plan dealt with the desirability of studying various physical phenomena during the flight experiment.

This report describes the effort funded by NASA ARC under contract NAS 2-8665 during which time a Flight Experiment Physical Phenomena Experiment Chest concept was generated. This concept is capable of demonstrating, using water, the following physical phenomena during a zero gravity flight experiment and at one gravity for comparative purposes:

A. Zero gravity liquid/solid interface progression.

B. Zero gravity melting/freezing temperature and latent heat of fusion.

C. Zero gravity supercooling effects.

D. Zero gravity convection from thermally induced surface tension changes.

E. Zero gravity boiling temperature and latent heat of evaporation.

F. Zero gravity wicking rate, wick wetting characteristics, and wick dryout characteristics.

SUMMARY

The objective of the Flight Experiment Physical Phenomena Chest portion of the Ice Pack Heat Sink Subsystem program is to generate a Flight Experiment Physical Phenomena Experiment Chest concept capable of investigating and demonstrating, using water, the following ice pack related physical phenomena during a zero gravity flight experiment:

A. Zero gravity liquid/solid interface progression.

B. Zero gravity melting/freezing temperature and latent heat of fusion.

C. Zero gravity supercooling effects.

D. Zero gravity convection from thermally induced surface tension changes.

E. Zero gravity boiling temperature and latent heat of evaporation.

F. Zero gravity wicking rate, wick wetting characteristics, and wick dryout characteristics.

A literature survey was performed to obtain material previously published relating to zero and low gravity studies of ice pack related physical phenomena. A total of eighty-one documents were selected for acquisition and review.

Utilizing the background information generated during the literature survey, a Flight Experiment Physical Phenomena Experiment Chest concept has been generated to investigate and demonstrate the physical phenomena listed in the objective above, a complete description of which is contained in this report. Additionally, detailed drawings, Physical Phenomena Experiment Chest-Schematic, SVSK 91539 sheets 1 and 2, and Physical Phenomena Experiment Chest - Hardware Arrangement, SVSK 91585 sheets 1, 2, 3, and 4 have been prepared and transmitted under separate cover.

Based on the results of this program, the Flight experiment Physical Phenomena Experiment Chest concept has been developed to be an acceptable concept for a zero gravity flight experiment.

CONCLUSIONS

Completion of the Flight Experiment Physical Phenomena Experiment Chest portion of the Prototype Ice Pack Heat Sink Subsystem program has led to the generation of an experiment chest concept capable of investigating and demonstrating the six categories of ice pack related physical phenomena.

An assessment of the appropriateness of each experiment has produced the following conclusions:

EXPERIMENTS OFFERING SIGNIFICANT SCIENTIFIC/ENGINEERING ACHIEVEMENT:

C. Zero gravity supercooling effects.

D. Zero gravity convection from thermally induced surface tension changes.

F-1. Zero gravity wicking rates.

F-3. Zero gravity wick dryout characteristics.

EXPERIMENTS OFFERING MINIMAL SCIENTIFIC/ENGINEERING ACHIEVEMENT:

A. Zero gravity liquid/solid interface progression.

B. Zero gravity melting/freezing temperature and latent heat of fusion.

E. Zero gravity boiling temperature and latent heat of evaporation.

F-2. Zero gravity wick wetting characteristics.

RECOMMENDATIONS

The effort expended during this program has evolved the following recommendations.

Four experiments offer potential for significant scientific/engineering achievement and each should be pursued as individual flight experiments:

C. Zero gravity supercooling effects.

D. Zero gravity convection from thermally induced surface tension changes.

F-1. Zero gravity wicking rates.

F-3. Zero gravity wick dryout characteristics.

Four experiments offer minimal potential for scientific/engineering achievement and further effort on each should be discontinued:

A. Zero gravity liquid/solid interface progression.

B. Zero gravity melting/freezing temperature and latent heat of fusion.

E. Zero gravity boiling temperature and latent heat of evaporation.

F-2. Zero gravity wick wetting characteristics.

The experiment Chest should be repackaged to include only those experiments deemed appropriate for implementation.

NOMENCLATURE

A	Area
At	Throat area
a	Width
atm	Atmosphere
C	Capacitance
C_D	Discharge coefficient
C_p	Specific heat
^0C	Degrees Celsius
cm	Centimeter
D, D_c, D_w	Dielectric constant
d	Diameter, thickness
d*	Throat diameter
E_s	Streaming potential
g	Gram, gravitation constant
H_f	Heat of fusion
$\Delta\Delta H_f$	Error in heat of fusion
H_v	Heat of vaporization
$\Delta\Delta H_v$	Error in heat of vaporization
H_2O	Water
h, h_o, h_i, h_w	Height, thickness
hr	Hour
in	Inch
J	Joule
K	Degrees Kelvin, thermal conductivity
$K/\Delta x$	Thermal conductivity rate
k, k_1, k_2	Thermal conductivity
kg	Kilogram
kPa	Kilopascal
kJ	Kilojoule
Δk	Error in thermal conductivity
L	Total length
ℓ	Wetted length
M_w	Molecular weight
m, $\dot{m}$	Mass flow rate, meter
mm	Millimeter
min	Minute

NOMENCLATURE (CONT.)

m_i	Mass of ice
mW	Milliwatt
$\bar{m}$	Mass
N	Newton
n	Number of capillaries
P, Po, Pe, P_1, P_2	Pressure, vapor pressure
Pc	Chamber pressure
Pt	Platinum
Pw, Pw_1, Pw_2	Wick pressure
ΔP	Pressure differential
Pa	Pascal
pF	Picofarad
psi	Pressure in pounds per square inch
Q	Heat transfer rate
$\dot{q}$	Heat flow
R, R′	Gas constant
r	Radius
r_w	Wick average capillary radius
s, sec	Second
T, To, T_1, T_2	Temperature
T_b	Temperature at bottom
T_c	Chamber temperature
T_f	Final temperature
T_i	Initial temperature
T_t	Temperature at top
T. C.	Thermocouple
ΔT	Temperature differential, error in temperature measurement, deviation in tempeature
ΔT_m	Melting temperature change
$\Delta T/\Delta x$	Thermal gradient
dT/dt	Rate of change of temperature
t	Time interval
Δt	Time interval differential, error in time interval
V	Volume, voltage
V_g	Gas volume
V_l	Liquid volume
dV/dt	Flow rate
W	Watt
$\bar{W}$	Steady state heat transfer rate
W_t	Total heat input
ΔW	Heat input differential

NOMENCLATURE (CONT.)

x	Thermal path length
Γ	Convenient constant
γ	Surface tension, specific heat rate
ϵ_0	Permissivity
ζ	Zeta potential
η	Viscosity
θ	Interfacial contact angle
λ	Specific conductance
$\rho, \rho_1, \rho_2, \rho_n$	Density

ZERO AND LOW GRAVITY LITERATURE SURVEY

In order to generate background information to be utilized in developing the physical phenomenon concepts, a literature survey to obtain material previously published relating to zero and low gravity studies of ice pack related physical phenomena was performed.

An in-house search was completed covering the period from January 1965 through January 1975 utilizing the following sources:

American Institute of Aeronautics and Astronautics Index

Applied Science and Technology Index

International Aerospace Abstracts

Scientific and Technical Aerospace Reports

In addition, the following two searches conducted by NASA Scientific and Technical Information Office, covering the period from January 1968 to March 1975, were reviewed:

NASA Literature Search No. 28737 - Fluids in Zero or Low Gravity Conditions

NASA Literature Search No. 28738 - Weightlessness

Eighty-one citations were selected for acquistion and review, and are listed in Appendix A. Of particular interest was reference 32, "Natural Convection in Low G Environments", which summarizes the results of convective experiments performed during the Apollo 14, 16, 17, and Skylab space flights; reference 52, "The Freezing of Supercooled Water", which describes efforts to produce nuclei-free water for supercooling studies; and reference 54, "MSFC Skylab Corollary Experiment Systems Mission Evaluation", which summarizes the various experiments performed in zero gravity during the Skylab flights. Many of the other references provided particular insights that were valuable in the concepting of our particular experiments.

We were particularly concerned with producing a series of experiments that do not duplicate previously performed effort; the background derived from the documents uncovered during our literature search has enabled us to satisfy this objective.

PHYSICAL PHENOMENA EXPERIMENT CHEST CONCEPT

Utilizing the background information generated during the literature survey task, a Flight Experiment Physical Phenomena Experiment Chest has been concepted to demonstrate the following physical phenomena during a zero gravity flight experiment:

A. Zero gravity liquid/solid interface progression.

B. Zero gravity melting/freezing temperature and latent heat of fusion.

C. Zero gravity supercooling effects.

D. Zero gravity convection from thermally induced surface. tension changes.

E. Zero gravity boiling temperature and latent heat of evaporation.

F. Zero gravity wicking rate, wick wetting characteristics, and wick dryout characteristics.

In the following sections each phenomenon is described and the method of observation and evaluation of each is presented.

Each experiment described investigates and demonstrates physical phenomena directly associated with the Ice Pack Heat Sink Subsystem normal mode (freeze/thaw) and emergency mode (boiling) operation, and as such performs a necessary function in allowing complete understanding and, therefore, predictability of Ice Pack zero gravity operation. Further, each of these experiments provides additional insight into the zero gravity physical actions of the phenomena as related to potential applications other than the Ice Pack. Included is an assessment of the appropriateness of each experiment with respect to previous zero gravity activity and potential scientific/engineering accomplishments.

A. ZERO GRAVITY LIQUID/SOLID INTERFACE PROGRESSION

Objective

The objective of this module is to investigate the configuration of a water/ice interface in a volume of water progressively freezing in a zero gravity field. The nature of this experiment is such that it can be developed in a one gravity environment where natural convection occurs and the results compared to the zero gravity results where convection is induced only by surface tension gradients.

Description of Experiment

The experiment is performed by chilling a quantity of water from one side and controlling the rate of cooling to establish a slowly progressing water/ice interface that can be observed visually.

The basic module is a deaerated, water filled, cylindrical container as shown in Figure 1. The inside diameter of the cylinder is large compared to the height to avoid edge effects. The bottom end of the cylinder is a flat copper plate to provide good heat transfer, and the top is an optically flat glass plate to allow observation of the water/ice interface. The side of the cylinder is insulated to minimize heat transfer in the radial direction. A fill port, which incorporates an expansion device, is located near the top of the cylinder. A thermoelectric device provides cooling to the bottom copper plate, and the top surface is maintained at ambient temperature. A camera is used to monitor the water/ice interface configuration at appropriate time intervals, and suitable lighting is provided to give optimum interface definition and depth of field.

The experiment will be conducted at two different cooling rates by maintaining the copper plate at constant temperatures of -5 ^{o}C and -15 ^{o}C while the top plate is exposed to an ambient temperature of 21 ^{o}C.

Analytical Investigation

The heat transfer rate at steady state condition is given by

$$\bar{W} = \frac{\pi d^2 (k_2 T_2 - k_1 T_1)}{4h}$$

(Refer to Appendix B for derivation of equation)

where $\bar{W}$ = steady state heat transfer rate in watts

d = diameter of cylinder = 12.7 cm

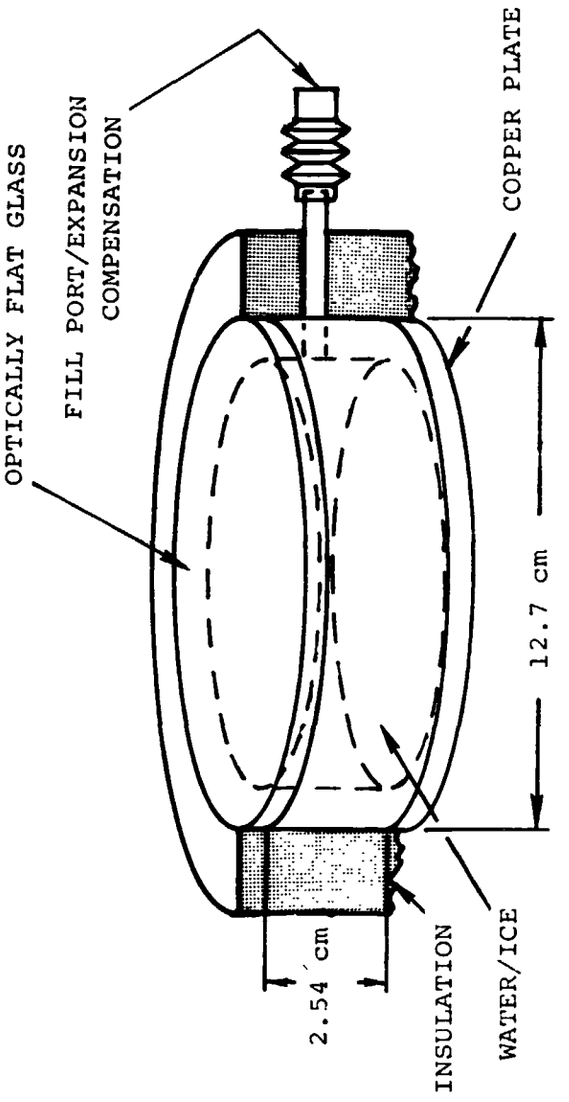

FIGURE 1: ZERO GRAVITY LIQUID/SOLID INTERFACE PROGRESSION MODULE

h = height of cylinder = 2.54 cm

k_2 = thermal conductivity of water = 5.9×10^{-3} W/cm^{o}C

k_1 = thermal conductivity of ice = 22.5×10^{-3} W/cm^{o}C

T_2 = ambient temperature = 21 ^{o}C

T_1 = cold plate temperature = -5 ^{o}C and -15 ^{o}C

The maximum steady state heat transfer rate at T_1 = -15^{o}C is 23 W and the ice water interface position as given by

$$h_o = \frac{-k_1 \pi d^2 T_1}{4 \bar{W}}$$

is 1.86 cm from the bottom plate. The minimum steady state axial heat transfer rate at T_1 = -5^{o}C is 11.8 W, and the interface is located 1.21 cm from the bottom plate.

In order to minimize edge effects, the radial heat transfer should be less than 0.01 times the axial heat transfer or less than 0.118W. Since the ice water interface will progress a maximum of 1.86 cm, the depth of field for the camera system should be a minimum of 2 cm.

The heat removal required to bring the water from 21^{o}C to steady state at T_1 = -15^{o}C is 106.9 kJ, and the average heat loss rate, axial and radial, is 12 W, approximately one half the steady state rate, which over a 10 minute period would be 7.2 kJ for a total heat removal of 114 kJ. The average heat removal rate requirement to reach steady state in 10 minutes is, therefore, 190 W.

Component Specifications

Container

Cylinder - 12.7 cm internal diameter, 2.54 cm high.

Top - optically flat glass of sufficient thickness to withstand a ΔP of 103 kPa (15 psi).

Bottom - 0.635 cm copper plate (plated to prevent corrosion)

Insulation - sufficient to give less than 0.1 W heat loss at T = 35^{o}C

Fill Port - 0.635 cm internal diameter

Expansion Diaphragm - to withstand a ΔP of 103 kPa (15 psi); maximum expansion of diaphragm = 1 cm^3.

Seals - to prevent leakage at ΔP = 103 kPa (15 psi).

Heat Sink (Source)

Thermoelectric cooler - Surface temperature controlled to ± 0.5 °C down to -16 °C. Minimum cooling power = 200 W.

Data Acquisition

Camera

Minimum depth of field at f/16 = 2 cm.
Minimum field of view = 5 cm diameter.
Minimum height resolution = 1 mm.

Lighting intensity sufficient for maximum exposure time of 1 s at f/16.

Automatic exposure at 30 s intervals.

Hardware Description

Figure 2 shows the configuration of Experiment A, Zero Gravity Liquid/Solid Interface Progression. The water sample to be frozen is contained within a low thermal conductivity teflon cylinder by an optically flat glass plate and a copper plate sealed with elastromeric "O' rings. The copper plate is tin plated to prevent corrosion and to allow attachment of thirty thermoelectric cooling units (Melcor CP 1.4-71-06) which cool and freeze the water sample during the experiment. These cooling units are arranged electrically in 6 circuits of 5 units each in series in order to match their operating voltage to a 28 VDC supply voltage. Each circuit is switched separately to keep the switched current to a value that can be handled by solid state devices. Two platinum resistance temperature sensors attached to the copper plate provide surface temperature inputs to the control box. A tin plated stainless steel plate/fin heat exchanger is soldered to the hot side of the thermoelectric devices to effectively remove the generated heat. Cooling water is admitted to the heat exchanger thru a Valcor P/N V27200-520 latching solenoid valve that is being used on Hamilton Standard's Water Boiler Thermal Control Hydraulic program for the Shuttle Orbiter. This same valve is used throughout all the experiments for on-off water and vacuum control. A thermal expansion compensation stainless steel bellows is attached to the teflon cylinder to accommodate the volume change as the water freezes. A limit switch with integral connector senses the position of the bellows and sends a signal

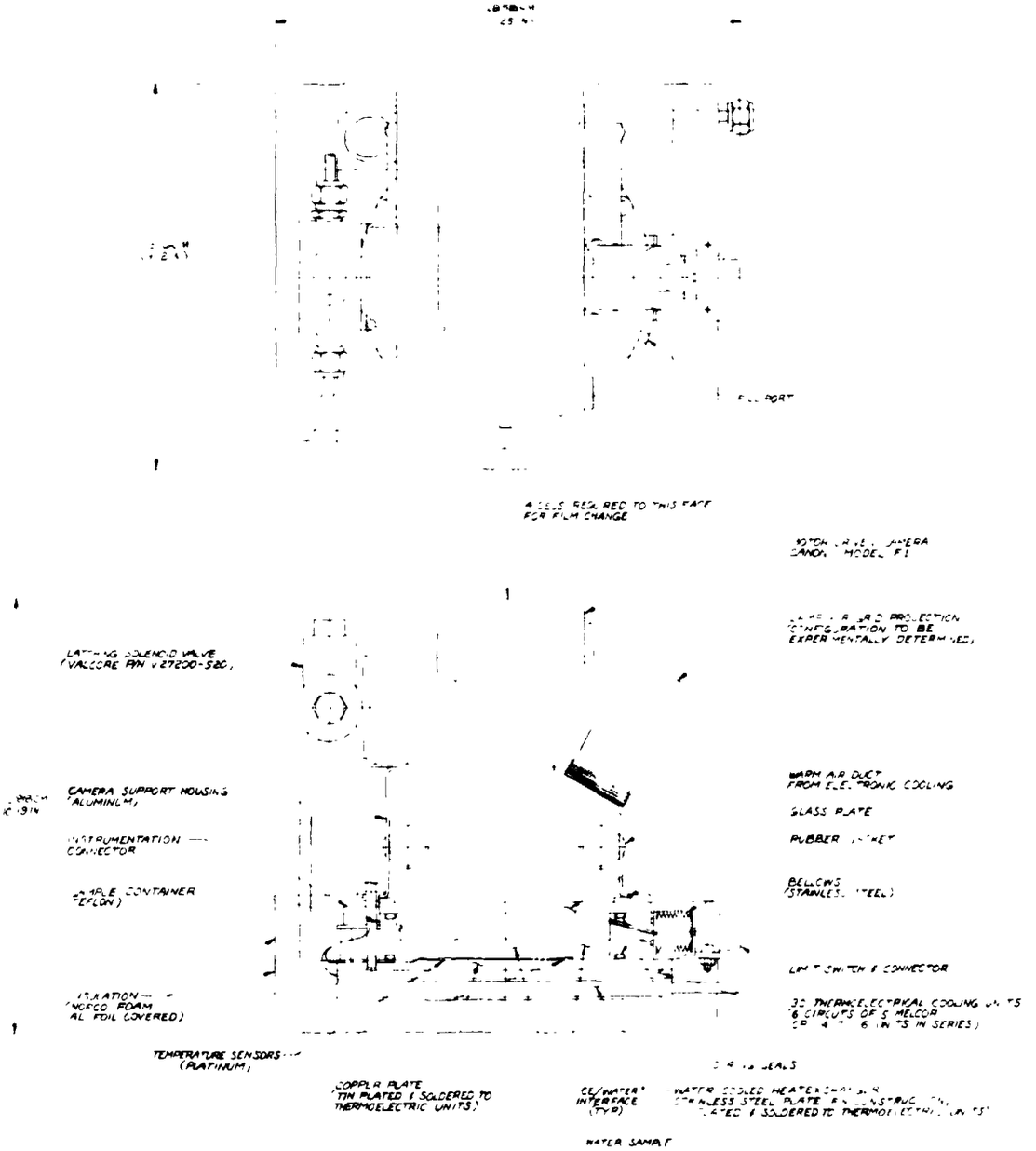

FIGURE 2

EXPERIMENT A ZERO GRAVITY LIQUID SOLID INTERFACE PROGRESSION HARDWARE ARRANGEMENT

to shut dowr the experiment if the ice layer gets too thick. Normally the ice layer thickness is self limiting, due to the insulating effect of the ice layer, to a thickness that will not actuate the switch. A fill port is located in the teflon cylinder wall. Nopco foam insulation covered with aluminum foil tape to meet spacecraft fire criteria, used through the ice pack experiment, surrounds the sample container and cooling equipment to reduce heat loss and eliminate condensation. Six bolts threaded into the copper plate attach an aluminum camera support housing to the assembly and hold the glass plate to the sample container with a rubber gasket. A motor driven Canon model F1 camera, a lighting fixture, and the water valve are attached to this housing. The proposed lighting technique utilizes a lamp and a grid projection lens system that allows the camera to photograph the image of the grid as it is reflected from the two surfaces of the glass and from the ice/water interface. As the ice/water interface progresses, its location is determined from the shift of the ice grid reflection with respect to the two fixed glass reflections The general shape of the ice surface is determined from the distorted characteristics of the ice grid reflection. The optimum lighting technique must be determined experimentally.

The camera is motor driven and electrically actuated to allow it to be operated automatically by the system sequence controller. Access is provided to the back of the camera for film replacement by the vehicle crew.

Experiment Sequence

Experiment A is operated as follows:

a. Activate solenoid valve to begin cooling of heat exchanger.

b. Energize thermoelectric cooling units.

c. Monitor temperature of copper plate.

d. At copper plate temperature of 0 ^{o}C begin camera/light sequence timer to take pictures every 30 seconds.

e. At copper plate temperature of -5 ^{o}C activate temperature control circuit.

f. After 15 minutes, stop camera and turn off thermoelectric units.

g. Allow cooling water flow to heat unit and thaw ice.

h. At +15 ^{o}C copper plate temperature, repeat steps b, thru f, except in step e, control copper plate temperature at -15 ^{o}C.

i. Turn off all equipment.

Appropriateness of Experiment

This experiment is intended to uncover any anomolies that may occur at the liquid/solid interface as water freezes in a zero gravity environment. The existence of a cellular suface tension circulation pattern, "Benard Cells", has been demonstrated during Skylab experimentation (reference 32, Appendix A) and it is speculated that peculiar interface configurations could occur. However, the shape of the interface is not apt to vary significantly from the one gravity shape and, in any event, would not be of magnitude to cause a significant varience in any known space application. Therefore it is concluded that this experiment must be treated as having only academic interest.

B. ZERO GRAVITY MELTING/FREEZING TEMPERATURE AND LATENT HEAT OF FUSION

Objectives

The two objectives of this module are to determine the melting/freezing temperature and the latent heat of fusion of water in a zero gravity field. The measurements will be made on bulk water and water contained within a dacron wick media. The nature of this experiment is such that it can be developed in a one gravity environment and the results compared to the zero gravity results. Analysis indicates that a measurable difference in melting point and latent heat of fusion is not to be expected between zero g and one g.

Description of Experiment

To run the experiment, water is frozen at -5°C by sublimation of water sprayed on the sample container, and sufficient time, less than 30 minutes, is allowed for thermal gradients throughout the sample to dissipate. Heat is then supplied by a heater element at a constant rate ($\sim$ 1 watt), and the temperature at the center of the ice mass is measured as a function of time. Heating is discontinued when the temperature indicates melting is complete, and the final temperature is measured after the thermal gradients in the sample have dissipated ($dT/dt = 0$). From the temperature-time ($\sim Q$) plot the melting point and the latent heat of fusion can be determined after subtraction for the thermal mass of the container and surroundings. This subtraction factor can be predetermined by appropriate experiment and/or calculation and is independent of the gravity field.

The experimental module shown in Figure 3 is a cylindrical metal container, capacity 16 cm^3, with approximately 10 g of pure water, provided with three temperature sensors in the center. This design also accommodates the dacron wick material. The container is heated electrically with a constant one watt to melt the sample. Surrounding this element is another heater element in which the power is controlled automatically to maintain a ΔT of zero between T_1 and T_2. Thus, heat loss to the surroundings from the water container and the heater element is negligible.

Analytical Investigation

Effect of Gravity on Melting Point of Ice

The melting point of ice as a function of pressure can be determined from the pressure - temperature phase diagram for water, or from the triple point and the defined melting point at atmospheric pressure. The relation is:

HAMILTON STANDARD Division of UNITED TECHNOLOGIES

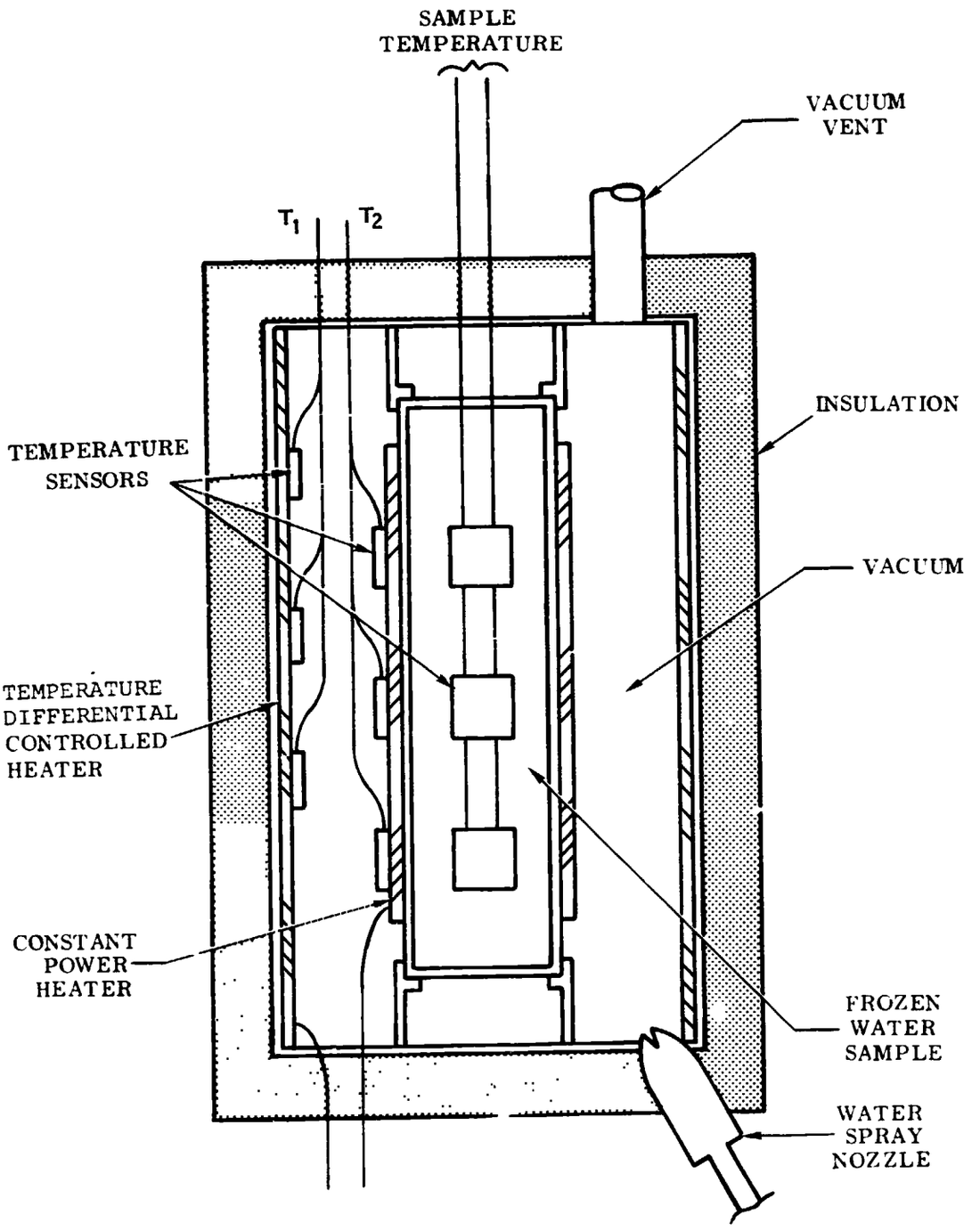

FIGURE 3 . ZERO GRAVITY MELTING/FREEZING TEMPERATURE AND LATENT HEAT OF FUSION MODULE

$$\frac{\Delta T_m}{\Delta P} = -7.45 \times 10^{-8}\ ^{o}C/p \quad \text{(slope of phase diagram for water)}$$

The pressure on a given mass due to a gravitational field will depend on the configuration of the mass and it's orientation in the field. Considering a 10g cylindrical mass of ice, e.g. 1 cm ^{2} x 10 cm, orientated in the force field as shown below, the

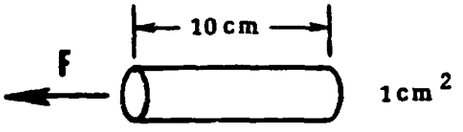

pressure at the bottom of the cylinder is

$$p = \frac{F}{A} = \frac{mg}{A} = 980\ Pa$$

The difference in melting temperature between the ice at the top of the cylinder (where the mass and therefore the force approaches zero) and the bottom is

$$\Delta T_m \approx -7.45 \times 10^{-8} \times 980 = -7.3 \times 10^{-5}\ ^{o}C$$

From this calculation it is anticipated that the difference in melting point of ice in a one vs. a zero-g field is extremely small.

Heater Power Requirements

It is desired that the 10 g sample of ice at -5 ^{o}C be melted within approximately one hour and that the final water temperature not exceed +10 ^{o}C.

A length equal to one half the container was modeled. This was divided into five concentric ring segments with the center ring containing 2 g, the next two rings having 1 g each and the two outer most rings containing ½ g each as shown in Table 1.

The reason differing masses of water were included in each ring was that the temperature slope was expected to be steeper in the region of the heat addition. The following physical properties were assumed:

Thermal Conductivity (K)

Node No.	Nodal & Location R (cm)	Thermal Mass (J/°C)		Heat of Fusion (J)	Sample Mass (g)
		Ice	Water		
1	.7308	1.05	2.1	167.0	0.5
2	.6914	1.05	2.1	167.0	0.5
3	.6265	2.10	4.2	334.0	1.0
4	.5288	2.10	4.2	334.0	1.0
5	.2629	4.20	8.4	668.0	2.0

Node I	Node J	Inter-Nodal Conductivity	
		(C_{I-J}) Ice	(J/s°C) Water
1	2	6.381	1.588
2	3	3.586	0.892
3	4	2.087	0.520
4	5	0.506	0.126

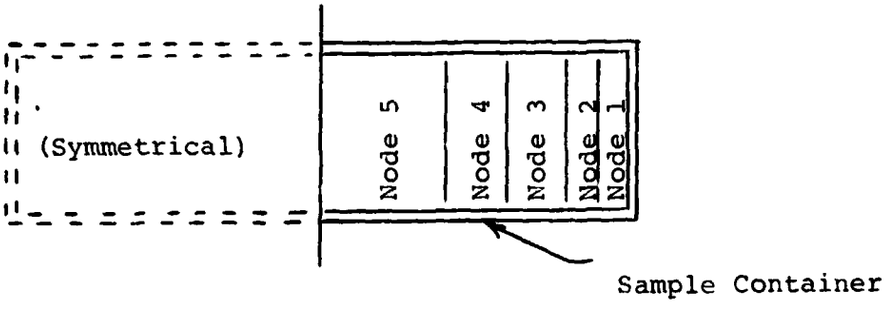

TABLE 1: INPUT DATA

For Ice $K = 2.25$ W/m°C
For Water $K = 0.59$ W/m°C

Specific Heat (Cp)

Ice Cp @-2.2 °C = 2.103 J/g°C
Water Cp @+2.0 °C = 4.214 J/g°C

Heat of Fusion (Hf)

Hf = 334 J/g

Ice properties were used for each mode until the heat input was equal to the latent heat of fusion for the mode. When this condition was met the properties were switched to those of water (liquid).

The problem was done by writing a short program in Super Basic Language and solving using the TYMSHARE computer system.

Cases were run for 2 W and 1 W of total applied heater power. The resulting temperature histogram for 1 W is presented in Figure 4. Figure 5 shows the temperature vs. time plot for 1 W heat input.

It is recommended that the applied power be limited to 1 W to avoid excessive temperature overshoots.

Error Analysis

The latent heat of fusion of ice will be determined by subtracting from the total heat input (W_t) the sum of the heat leakage, the energy required to raise the temperature of ice to the melting point, the water to the final temperature, and the container system from initial to final temperature $(T_f - T_i)(\Sigma_1^n m_i Cp_i)$. The probable error in the heat of fusion will be:

$$\Delta\Delta Hf = [W^2 \Delta t^2 + t^2 \Delta W^2 + 2 \Delta T^2 \Sigma_1^n (m_i Cp_i)^2]^{\frac{1}{2}}$$

Assuming the following values:

$t = 3600$ s $\quad \Delta t = 1$ s
$W = 1$ W $\quad \Delta W = 10^{-3}$ W
$\Sigma_1^n m_i C_{pi} = 218$ J/°C $\quad \Delta T = \frac{1}{5} \times 10^{-2}$ °C

$$\Delta\Delta Hf = [1 + 12.96 + 50 \times 4.75]^{\frac{1}{2}} = \pm 16 \text{ J}$$

The percent error is:

$$\frac{\Delta\Delta Hf \times 100}{Hf} = \frac{1600}{3340} = 0.48\%$$

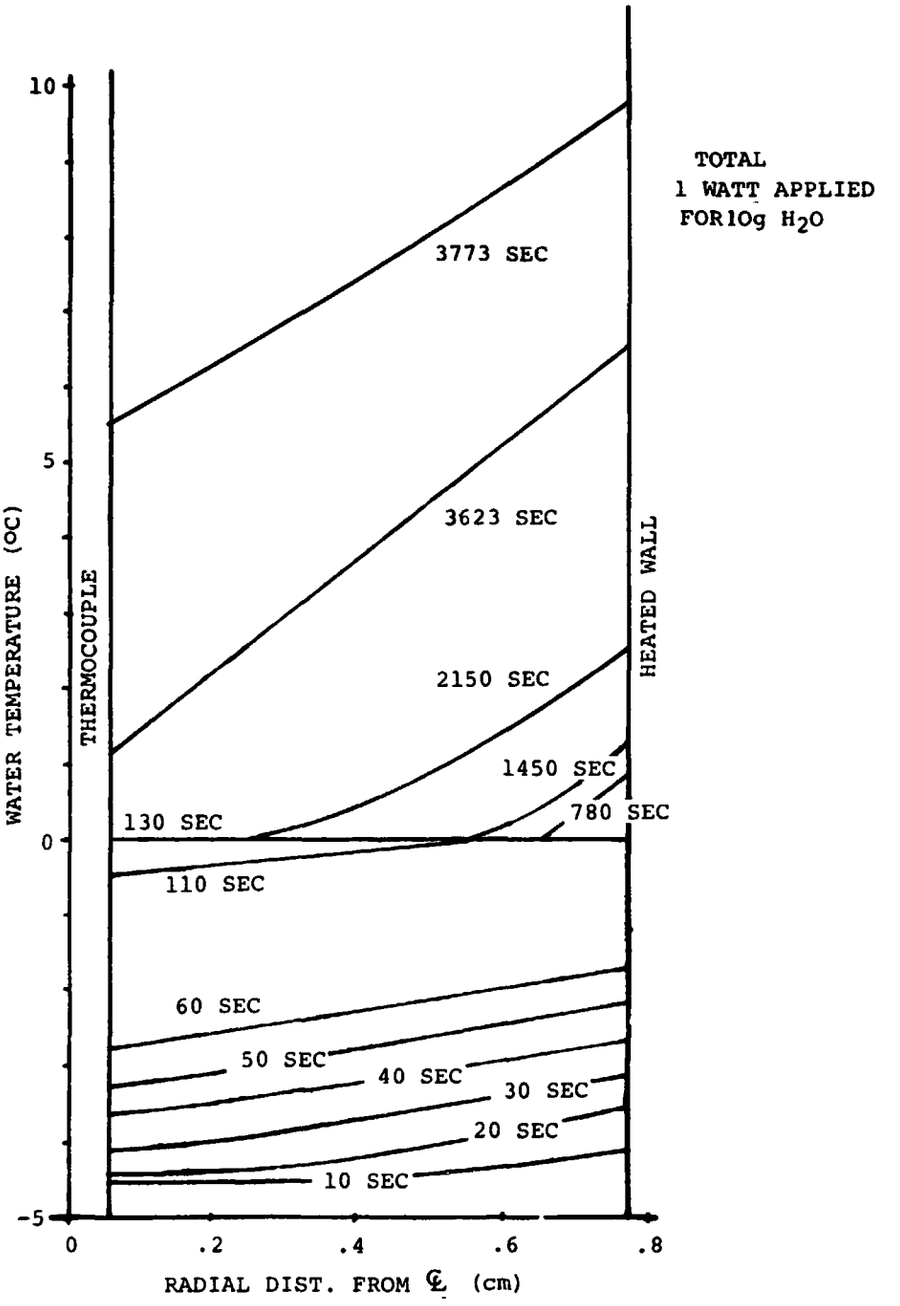

FIGURE 4: TEMPERATURE HISTOGRAM 1.0 WATTS APPLIED POWER

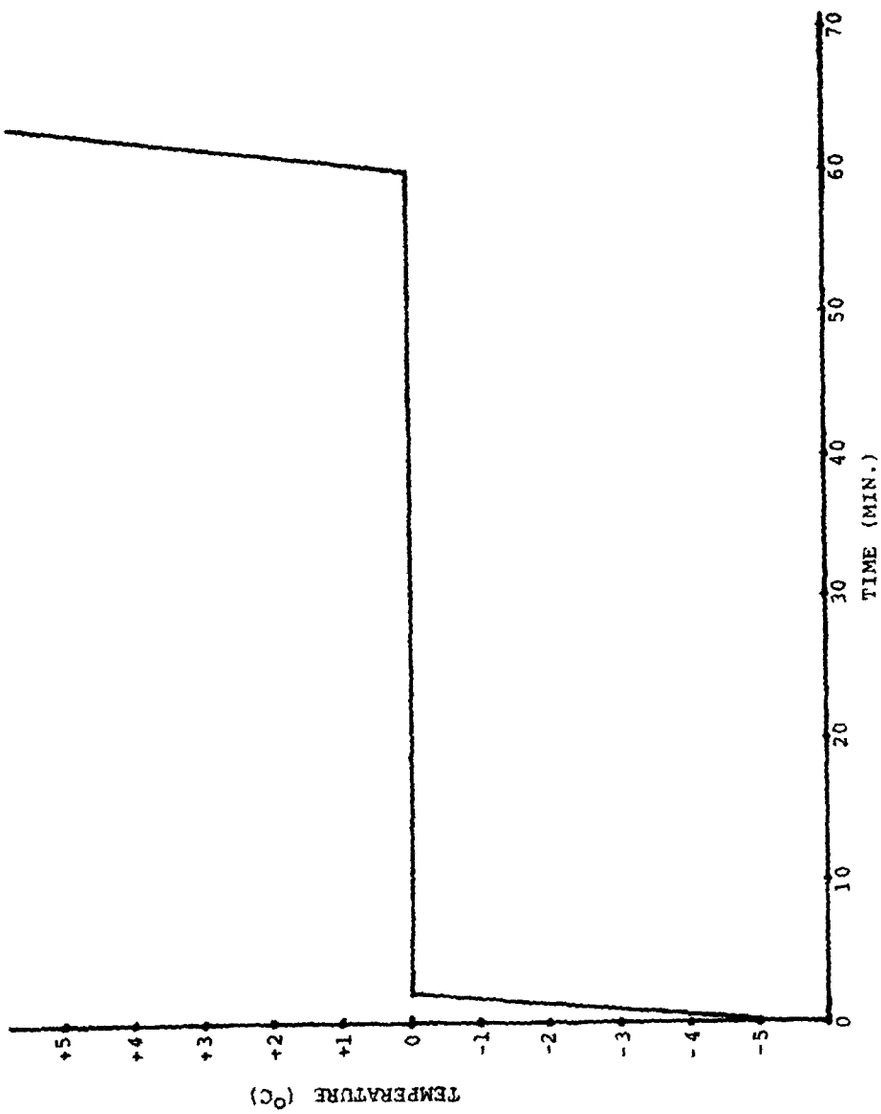

FIGURE 5: TEMPERATURE VS TIME PLOT 1.0 WATTS APPLIED POWER

The largest contribution to the probable error is the temperature measurement. If the temperature could be measured to $\pm$ 0.010 ^{o}C the probable error would be reduced to $\pm$4.85 or 0.14%.

Total Thermal Mass and Maximum Heat Leakage

The amount of heat energy required to raise the temperature of the system (10 g H_2O + 34 g Pt) from -5 ^{o}C to + 5 ^{o}C is 3.7 kJ. Added to this will be the thermal mass of the heater and the container and sensors. It will be assumed that the total heat energy required is 4 kJ. Since the error in the heat energy measurement is $\pm$ 16 J, the heat loss should be less than this value. A heat leakage rate of 1.5 x 10^{-3} W (5.4 J for one hr) is a reasonable value. The major heat loss will be from the temperature measuring systems.

Component Specifications

Container

Capacity 16 cm^3, 1.5 cm internal diameter, 8 cm height, 34 g weight. Platinum construction.

Heating Element

Controlled constant heating rate (1W $\pm$ 10^{-3} W) to be fabricated as integral part of container for optimum heat transfer.

Outer Heating Element

5 W $\pm$ 0.1 W to be controlled from temperature sensor signals.

Insulation

Sufficient for heat loss rate of less than 1 W.

Container Stand Offs

Minimum thermal mass (less than 2 J/^{o}C).

Air Gap Between Containers

1 to 1.5 cm, thermal mass at 0^{o}C and 1 atm less than 0.14 J/^{o}C.

Heater Control Temperature Sensors

Accurate to $\pm$ 0.1 ^{o}C

Sample Temperature Sensor

Accurate to $\pm$ 0.1 ^{o}C, readable and reproducible to $\pm$ 0.05 ^{o}C.

Heat Loss Rate (Including Sensors)

Less than 1.2×10^{-3} W.

Hardware Description

Experiment Bu (unwicked) and Bw (wicked) Zero Gravity Melting/ Freezing Temperature and Latent Heat of Fusion is shown in the Bu (unwicked) configuration in Figure 6 where the sample container is filled with a bulk water sample. In the Bw (wicked) version, the sample container is filled with dacron wick material that contains the water sample. In either case, the sample container is a platinum cylinder with wire supports that position three platinum probe temperature sensing elements centrally in the water sample. An "O" ring sealed cap encloses the sample and supports one end of the container on a teflon thermal standoff that minimizes heat transfer to and from the container. The other end of the container is similarly supported, and also includes an epoxy sealed temperature sensor wire lead feed through.

The constant rate heater is constructed as a silicone rubber enclosed resistance heating element bonded to the outer wall of the sample container. The temperature controlled heater is of similar construction, but is bonded to the inside wall of a stainless steel housing that encloses the sample container. Three platinum resistance temperature sensing elements are attached to each of the heater surfaces for controlling the temperature differential between the two heaters. A latching Valcor solenoid valve identical to that used in Experiment A connects the volume within the housing to an orificed overboard vacuum line. The vacuum causes freezing and subsequent sublimation of water sprayed onto the sample container resulting in freezing of the water sample inside the container. Cooling water spray is controlled by a pulsing and isolation valve being developed for the Shuttle Orbiter Flash Evaporator (Item 708). This valve will be fully developed for anti-freeze up, minimum dribble volume, cyclic response, and other features by the time the Ice Pack Experiment is built, and will incorporate a smaller, fan spray nozzle as the only modification for this experiment. The entire experiment housing is enclosed in aluminum foil covered Nopco foam insulation to minimize heat leakage.

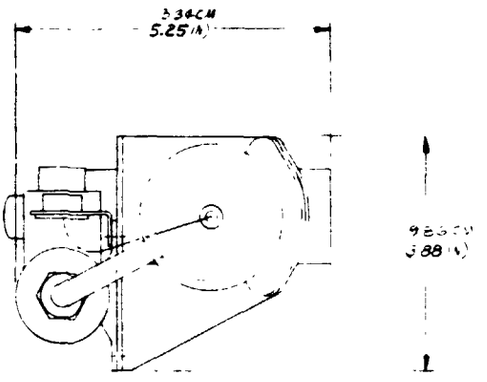

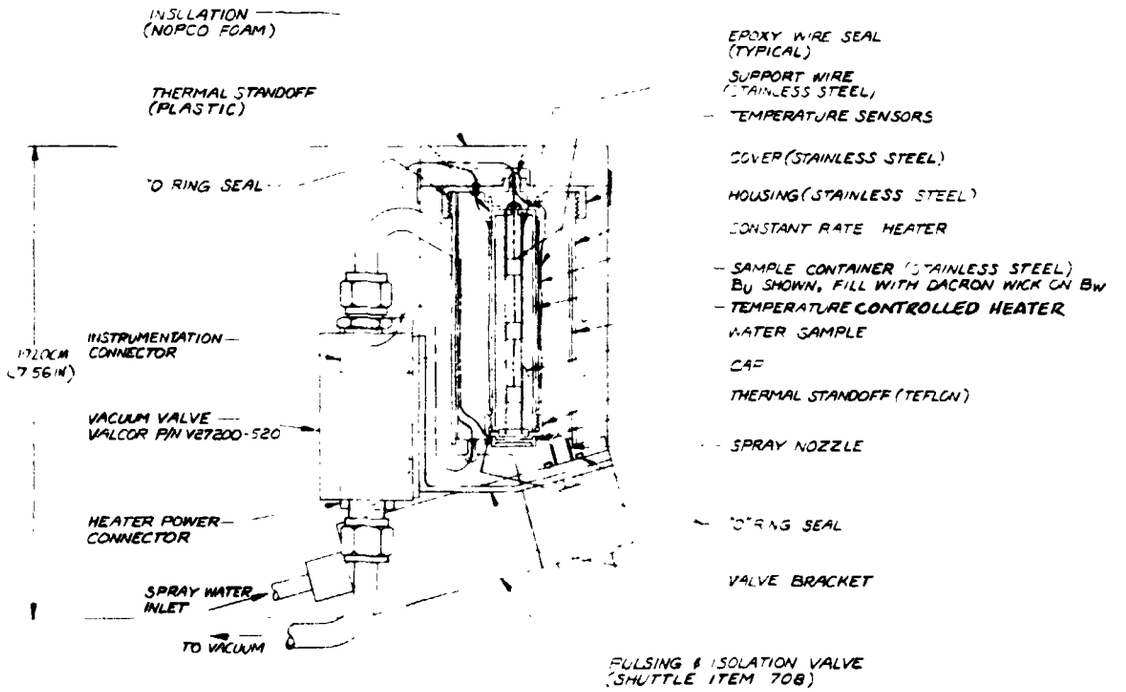

FIGURE 6. EXPERIMENT Bu AND Bw ZERO GRAVITY MELTING / FREEZING TEMPERATURE AND LATENT HEAT OF FUSION HARDWARE ARRANGEMENT

Experiment Sequence

Experiments Bu and Bw are operated as follows:

a. Open vacuum valve.

b. Turn on temperature sensing electronics.

c. Open isolation valve and begin operation of pulsing valve.

d. Turn off timed pulse and isolation valve when sample temperature reaches -10 ^{o}C.

e. Turn on Temperature controlled heater to maximum power.

f. Turn heater off when constant rate heater mounted sensors read 0 ^{o}C (to remove ice from chamber).

g. Allow 30 minutes for temperature stabilization (all sensors equal within 0.05^{o}C).

h. Turn on constant rate heater circuit and temperature control heater circuit.

i. Record sample sensor temperature every 30 seconds until temperature reaches +10 ^{0}C.

j. Turn off heaters and allow 30 minutes for temperature stabilization (continue recording sample temperature).

k. Stop recording temperature.

l. Turn off equipment.

Appropriateness of Experiment

This experiment is intended to determine the change in freezing point of water in a zero gravity environment compared to a one gravity environment, and to determine the change in the latent heat of fusion of water in a zero gravity environment compared to a one gravity environment. Analysis has shown that the change in freezing temperature will be on the order of 10^{-4} ^{o}C, a value that is quite insignificant. No reasons exist to expect a significant change in the latent heat of fusion of water, and experimental verification can be implied since performance durations vs. water usage of porous plate sublimators during zero gravity usage have been as expected. Therefore, it is concluded that this experiment must be treated as having little scientific necessity.

C. ZERO GRAVITY SUPERCOOLING EFFECTS

Objective

The objective of this module is to determine the effect of a gravitational field on the supercooling of ultra pure water. The experiment is to be conducted in one and zero gravity, and the results compared.

Description of Experiment

The sample of ultra pure water is enclosed in a cylindrical element cell with central temperature sensing as shown in Figure 7. All components in contact with the water are made from Teflon (non-wettable) to minimize nucleation sites, and special precautions are taken to remove impurities from the system prior to sealing the cell. The main body of the cell is thin wall Teflon to allow for volume changes and give good heat transfer rates.

The cell is positioned within a temperature controlled chamber. A suitable heat transfer liquid (Flutec PP50) fills the space between the cell and the thermoelectric element in the wall of a container surrounded by suitable insulation. A bellows device accommodates volume changes in the heat transfer fluid. Flutec PP50 was chosen as the heat transfer fluid because of its low toxicity, low melting point (-130°C), and relatively high boiling point (29°C at one atm), and its acceptability for use in a spacecraft cabin. The thermoelectric element is programmed to cool the heat transfer fluid at a constant rate, and the point at which freezing occurs is determined by the inflection in the sample temperature versus time plot.

Water purification and cell cleaning will be carried out in the same operation by placing the cell in the final stage of the triple distillation system. The basic cleaning procedure is via purified steam. All stages of the distillation system will contain platinum black for impurity absorption, boiling nucleation, and catalytic oxidation of impurities. The first distillation will be from basic permanganate solution. After sufficient steam-out of the purification system, the cell exit will be plugged and the purified water condensed directly in the cell. When the cell is completely filled with water, the inlet will be sealed and the cell transferred to the temperature controlled chamber.

To carry out the experiment, the thermoelectric element is programmed to cool the heat transfer fluid at the rate of 0.5 ± 0.05 °C per minute and a water temperature vs. time plot is generated. The temperature of freezing is determined by the inflection in the water temperature vs. time plot due to the latent heat of fusion.

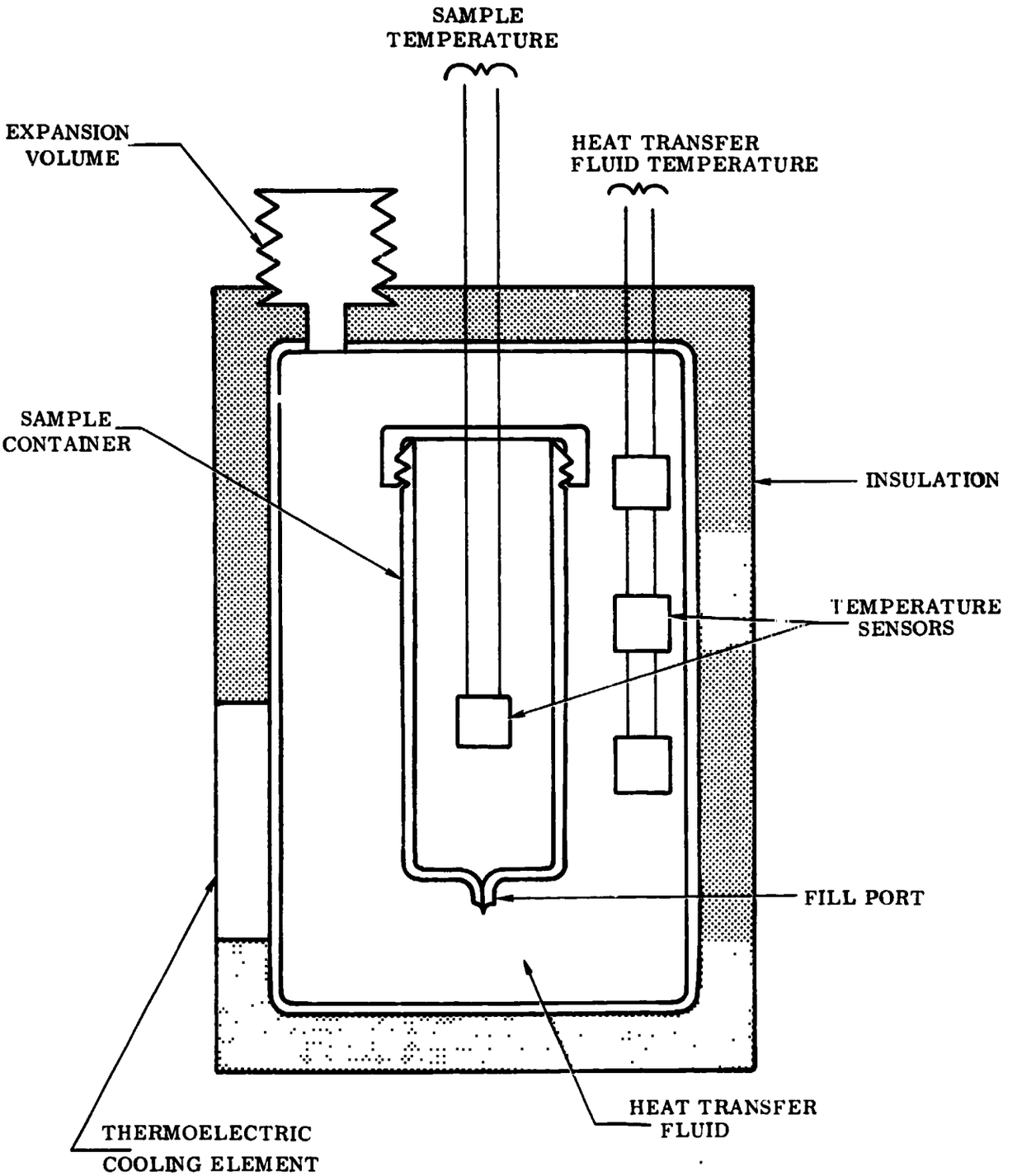

FIGURE 7: ZERO GRAVITY SUPER COOLING EFFECTS MODULE

The experiment can be repeated any number of times by reversing the current to the thermoelectric element and melting the sample.

Analytical Investigation

Volume of H_2O

$$V = \frac{\pi d^2 h}{4} = \frac{3.2\pi}{4} = 2.5 \text{ cm}^3$$

Volume of Flutec PP50

$V = V$ container $- V H_2O$ cell

$V = \pi(1.75 - 1)^2 \, 10.5 = 18.6 \text{ cm}^3$

Total thermal mass

$$2.5 \text{ g} \times 4.2 \text{ J/g}^{\circ}\text{C} + 18.6 \text{ g} \times 0.248 \times 4.2 \text{ J/g}^{\circ}\text{C} = 29.9 \text{ J/}^{\circ}\text{C}$$

Power

$$\frac{29.9 \text{ J/}^{\circ}\text{C} \times -0.5 \, ^{\circ}\text{C}}{60\text{s}} = -0.25 \text{ W}$$

Components Specification

Cell

Teflon/water only interface on inside, 1 cm internal diameter x 3.2 cm internal length. External length 10.5 cm.

Temperature Sensor Range

Accurate to $\pm 0.05^{\circ}$C over +5 $^{\circ}$C to -50 $^{\circ}$C

Thermoelectric Unit

+5 watt capacity, +10 $^{\circ}$C to -50 $^{\circ}$C range with 20 $^{\circ}$C coolant temperature, programmable for constant dT/dt of 0.5 $^{\circ}$C per minute.

Heat Transfer Medium

Flutec PP50, 18.6 cm^3.

Chamber Insulation

2.54cm rockwool or equivalent to give less than 0.5 W heat transfer rate at T = 70 $^{\circ}$C.

Thermal Expansion Bellows

1 to 6 cm^3 capacity. Minimum pressure one atmosphere.

Hardware Description

Experiment C, Zero Gravity Supercooling Effects shown in Figure 8, has an all teflon sample container with a single teflon coated platinum resistance temperature sensing element supported on teflon coated wires. This all teflon interior prevents premature freezing of the water sample by eliminating nucleation sites. The sample container is supported by a stainless steel cover and the stainless steel housing that the cover encloses. The container volume is completely filled with ultra pure water condensed directly in the container as the third stage of a triple distillation system. After purging, the container top is sealed and the container filled. The fill port is then clamped and heat sealed with the container cylindrical walls squeezed slightly oval to allow for expansion as the ice freezes. The volume between the sample container and the housing is filled with Flutec PP 50 as a heat transport fluid. Volume expansion compensation for the transport fluid is contained in the cover in the form of a stainless steel spring loaded bellows. Flutec PP 50 was chosen as the only liquid other than water permitted in the inhabitable portions of the Shuttle vehicle and for its low freezing point and acceptable boiling point. The fluid is cooled at a constant rate by a two stage Cambion 801-1005-01 thermoelectric cooling unit soldered to a flat on the side of the housing. The units are capable of cooling to -49°C at 0.8 watts, and as low as -60.9°C at zero watts while rejecting heat to a plate-fin water cooled heat exchanger soldered to the hot junction of the unit. Three temperature sensors provide a fluid temperature input for the constant rate cooler control circuit while a magnetic stirrer provides constant circulation to assure uniform fluid temperature distribution. The cooling water flow is controlled by the common Valcor latching solenoid valve.

Experiment Sequence

Experiment C is operated as follows:

a. Turn on temperature sensing electronics.

b. Open cooling water valve.

c. Turn on thermoelectric cooling unit and cooling rate electronics to maximum cooling rate until both temperatures reach +3 °C then cool at 0.5 °C/min.

d. Turn on stirrer.

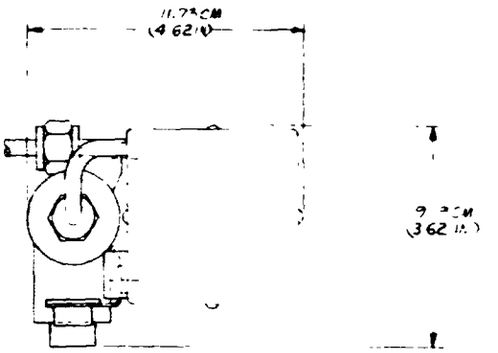

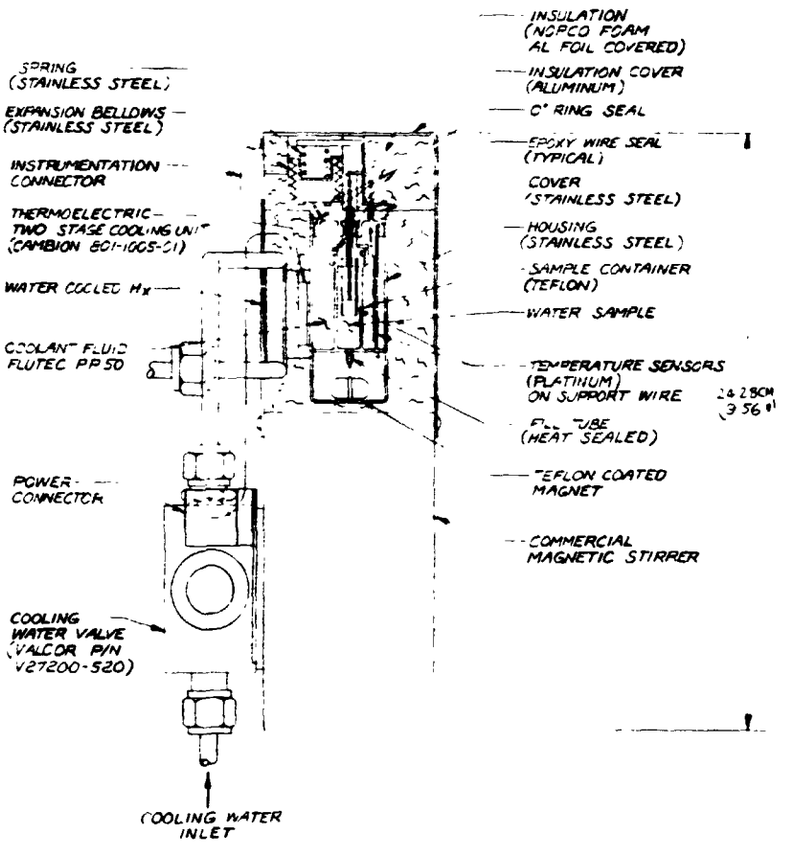

FIGURE 8: EXPERIMENT C ZERO GRAVITY SUPER COOLING EFFECTS HARDWARE ARRANGEMENT

e. Monitor sample temperature sensor and record temperature every minute.

f. Turn off data recorder, cooling rate control, and thermoelectric unit 5 minutes after sample temperature inflection.

g. Allow warmup to +3 ^{o}C with cooling water flow, then repeat c thru f as required.

h. Turn off equipment.

Appropriateness of Experiment

This experiment is intended to investigate differences in supercooling effects on ultra pure water between a one gravity environment and a zero gravity environment. Significant effort has been expended on investigating supercooling of water in a one gravity environment (reference 52, Appendix A), but no information could be obtained indicating any work had been done on zero gravity supercooling of water. Futher, since the prediction of quantitative results of supercooling in a one gravity environment is less than exact, speculation on zero gravity supercooling differences is not possible. Provisions must be incorporated to insure adequate vibration isolation during the conduct of the experiment.

Numerous pieces of space equipment exist that utilize water at or near the normal freezing temperature. A good understanding of zero gravity supercooling effects would undoubtedly allow more precise performance predictions for equipment operating in this temperature range. Therefore, it is concluded that a significant scientific advancement could be achieved by conducting a zero gravity supercooling experiment.

D. ZERO GRAVITY CONVECTION FROM THERMALLY INDUCED SURFACE TENSION CHANGES

Objective

The objective of this module is to make a quantitative study of heat transfer in bulk water and in water contained in a dacron wick to determine the contribution of surface tension convection to the overall heat transfer mechanism in a zero gravity environment.

Description of Experiment

The basic module shown in Figure 9 has two parallel discs 10 cm in diameter, one of which is a thermoelectric cooling device and the other is an electric heating element. The distance between the discs is 16 mm. Temperature sensors are located at 4 mm intervals to measure temperature gradient. One module is constructed to contain bulk water and a second module is constructed with dacron wick layers in the space between the discs.

A constant heat load ($\backsim$9 W) is applied by the heater while the heat pump maintains a fixed temperature gradient. Temperature sensors at various positions between the plates will detect any nonlinearities in the thermal gradient due to local convection currents. From the temperature measurements, the known heat transfer rate, and the dimensions of the module the thermal conductivity of water can be calculated. Deviations from the theoretical conductive value will indicate additional heat transfer caused by convection.

Analytical Investigation

Heat Transfer Rate ($\bar{W}$) from Conduction

The thermal conductivity of water at 22°C is 5.9 mW/cm°C so that

$$\bar{W} = \frac{6mW\ A\ \backslash T}{cm^{o}C\ \ \backslash X}$$

if $A = 25\pi$ cm^2 and X = 1.6 cm

$\bar{W} = 0.2945\ \backslash T$ W/°C

For a $\backslash T$ of 30 °C, $\bar{W} = 8.836$

Error Analysis

Assuming the cell dimensions are accurately known and constant the probable error in the thermal conductivity is given by

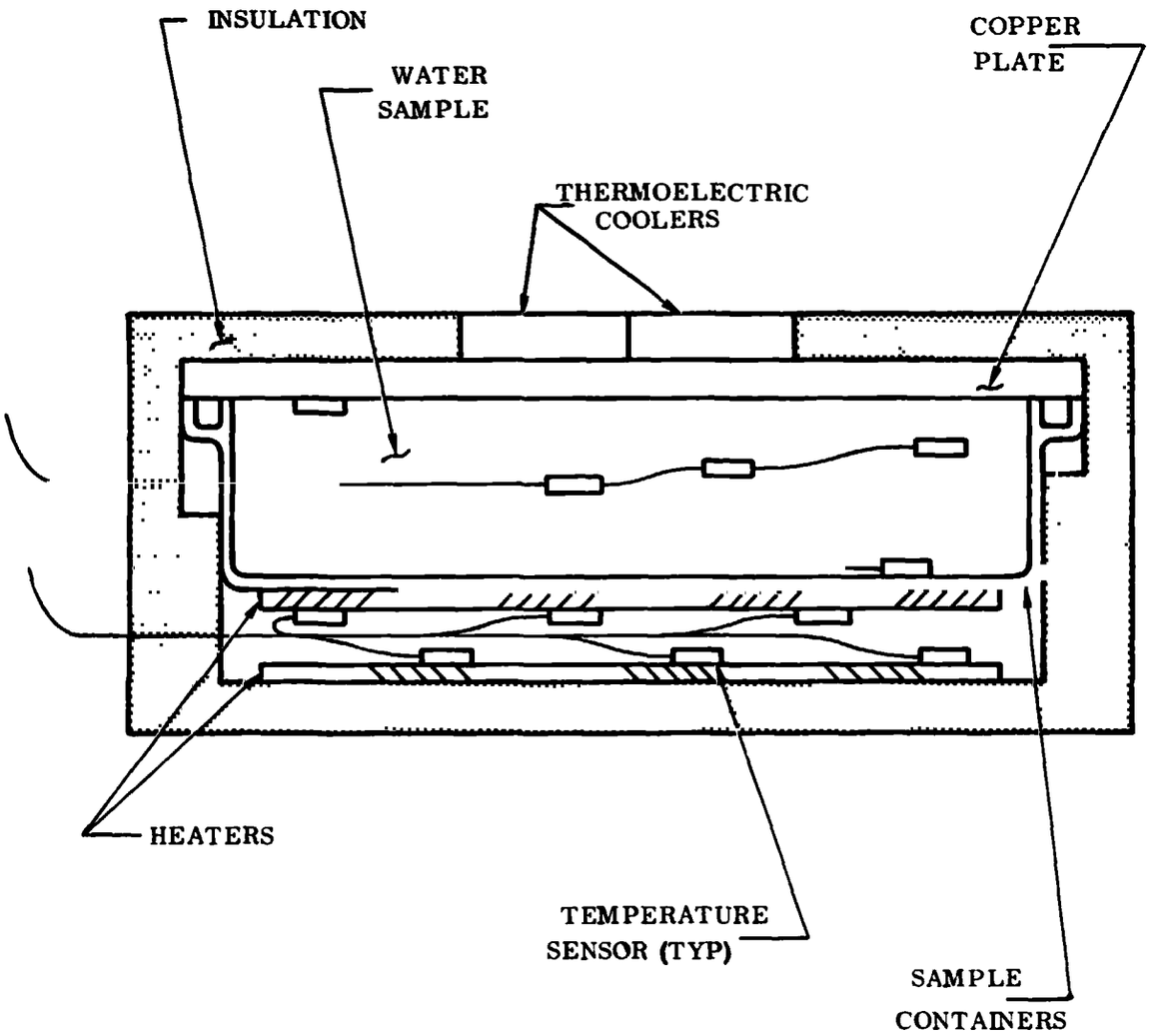

FIGURE 9 ZERO GRAVITY CONVECTION FROM THERMALLY INDUCED SURFACE TENSION CHANGES

$$\Delta k = \frac{0.02037}{cm(T_2-T_1)} \left[(\Delta\bar{W})^2 + \frac{2\bar{W}^2 (\Delta T)^2}{(T_2 - T_1)2} \right]^{\frac{1}{2}}$$

assume $\Delta T = \pm 0.1^{o}C$ $\quad (T_2 - T_1) = 30^{o}C$

$\Delta\bar{W} = \pm 10^{-2} W$ $\quad \bar{W} = 8,836$ W

$$\Delta k = \frac{0.679 \times 10^{-3} W}{cm\ ^{o}C} \left[10^{-4} + 17.35 \times 10^{-4} \right]^{\frac{1}{2}}$$

$$\Delta k = 2.906 \times 10^{-5} W/cm^{o}C$$

The percent error is $\frac{\Delta k \times 100}{k} = \frac{2.906 \times 10^{-3}}{6 \times 10^{-3}} = \pm 0.48\%$

Volume Change

The change in water volume in changing from an average system temperature of 22°C to a system ΔT of 30°C is obtained by comparing the weight of water in the cell (assuming constant cell volume) at a uniform temperature of 22°C with the weight of the same volume of water of variable density corresponding to a linear temperature gradient (7°C to 37°C) across the cell. The weight of water in any volume element is:

$$\Delta g = 25 \pi \rho \quad \Delta h = 12.5 \pi (\rho n + \rho n+1) \Delta h$$

The total weight is the sum of the weights of each volume element from h = o to h = 1.6 cm.

$$g = 12.5\pi \sum_{o}^{h} (\rho n + \rho n+1) \Delta h$$

Assuming a linear temperature gradient

$$\Delta h = \frac{1.6 \text{ cm } \Delta T}{30^{o}C} \qquad \text{or}$$

$$g = \frac{2.0944 \text{ cm}^3}{^{o}C} \sum (\rho n + \rho n+1) \Delta T$$

For a constant ΔT of 2.5°C

$$g = 5.236 \text{ cm}^3 [\rho o - \rho n + 1 + 2 (\rho_1 + \rho_2 + \ldots\ldots \rho n)]$$

where ρo is the water density at 7°C, ρ_1 the density at 9.5°C and $\rho n + 1$ the density at 37°C. Thus it is found that the weight of water in the system (125.664 cm^3) is 125.3386 g at a ΔT of 30°C whereas the weights of the same volume of water at a

uniform temperature of 22°C is 125.2857 g. Therefore the volume of water changes by -0.053 cm^3. This volume change can be accommodated by the flexing of the container walls.

Component Specifications

Constant Power Heating Element

10 cm diameter, controlled constant power 0 to 10 $\pm$ 0.01 W.

Temperature Controlled Heating Element

Maximum power 10 W, controlled so that $\Delta T \leq \pm 0.5$ °C.

Thermoelectric Cooling Unit

Maximum cooling power 10 W controlled by thermocouples so that $\Delta T \leq \pm 0.5$ °C.

Insulation

$k/\Delta x < 4$ mW/°C cm^2 for nominal 5 W load.

Sample Container

Flexible to accommodate volume change of $\pm$ 0.05 cm^3.

Temperature Sensor

Readable to $\pm$ 0.1 °C, accurate to $\pm$0.05°C, total heat loss rate less than 0.02 W.

Hardware Description

Experiment D, Zero Gravity Convection from Thermal Induced Surface Tension Changes is shown in the Du (unwicked) configuration in Figure 10 where a bulk water sample is contained within a thin cylindrical teflon sample container. Platinum resistance temperature sensing elements supported on wires attached to the side of the container are arranged at equal intervals between the ends of the cylindrical container. In the Dw (wicked) configuration these sensors are supported by layers of Dacron wick material that fills the container. In both cases one end of the container is sealed by an "O" ring against a tin plated copper plate to which two Melcor CP 1.4-71-06 thermoelectric cooling units have been soldered. A temperature sensing element is attached to the inside of the container end, and a constant power silicone rubber encased resistance heater element is bonded to the outside of the container end. A second heater is mounted on the inside of an insulation jacket that encloses the experiment. This heater is controlled to maintain a zero temperature differential between itself

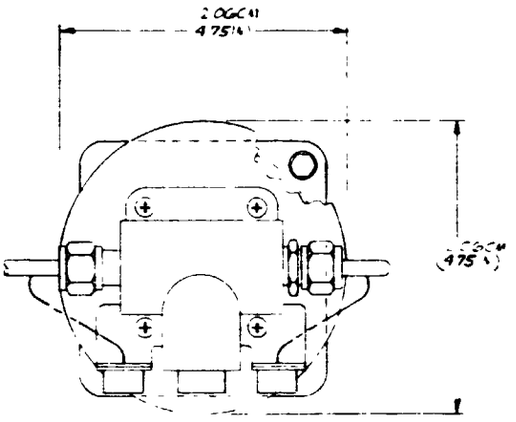

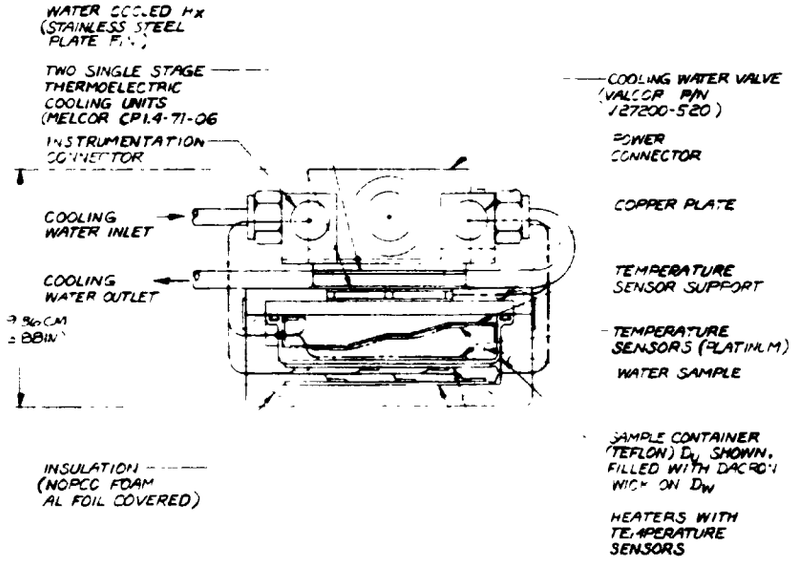

FIGURE 10:

EXPERIMENT Du AND Dw ZERO GRAVITY CONVECTION FROM THERMALLY INDUCED SURFACE TENSION CHANGES HARDWARE ARRANGEMENT

and the constant power heater, as sensed by temperature sensing elements mounted on both heaters, thereby eliminating heat loss from the back side of the constant power heater.

Experiment Sequence

Experiments Du and Dw are operated as follows:

a. Turn on temperature sensing electronics.

b. Open cooling water valve.

c. Turn on thermoelectric cooling unit and temperature control.

d. Turn on constant power heater.

e. Turn on zero temperature differential heater and control.

f. Record temperature at each sensor at one minute intervals for one hour.

g. Turn off equipment.

Appropriateness of Experiment

This experiment is intended to make a quantitative measurement of heat transfer in water in a zero gravity environment to assess the contribution of surface tension convection to the overall heat transfer rate. The existance of surface tension convection has been demonstrated during Skylab experimentation (reference 32, Appendix A) but no quantitative evaluation has been made. The fact that accurate heat transfer knowledge for zero gravity applications is essential cannot be denied. Therefore it is concluded that a significant engineering advancement can be achieved by measuring zero gravity convection from thermal induced surface tension changes.

E. ZERO GRAVITY BOILING TEMPERATURE AND LATENT HEAT OF VAPORIZATION

Objectives

The objectives of this module are to measure the boiling temperature and the latent heat of vaporization of pure water in unwicked and wicked media, and to compare the results of one gravity with those of zero gravity.

Description of Experiment

The vapor pressure of water in equilibrium with liquid water will be measured as a function of temperature over the range of 95°C to 105°C and the heat of vaporization H_v calculated using the Clapeyron-Clausius equation.

$$H_v = (Vg - V_l) \frac{dP}{d\ln T}$$

The boiling point can be determined by interpolation of the data to 1 atm pressure.

Containers with a volume of ~10 cm^3 fitted with a pressure transducer will hold the water and water-wick samples. These sample containers will be located in a uniform, controlled, temperature bath.

Each sample is prepared by placing approximately one gram of pure water into the sample container followed by evacuation of the container to remove entrained air. Before and after evacuation weights are taken to insure that at least 0.1 g but no more than 0.5 g of water remain in the container after air removel.

The sealed sample containers are placed in the uniform temperature bath and sample temperature - pressure readings taken over the temperature range 95 °C to 105 °C with sufficient time allowed to reach equilibrium at each temperature. Equilibrium conditions can be assumed when the bath and sample temperatures are equal to within $\pm$0.02 °C.

Analytical Investigation

Clapeyron-Clausius Equation

The latent heat of vaporization of a liquid is given by the Clapeyron-Clausius equation.

$$H_v = (V_g - V_l) \frac{dP}{d\ln T}$$

where V_g and V_l are the specific volume of vapor and liquid, respectively, and H_v the specific heat of vaporization. This equation can be arranged to give

$$V_g \frac{dP}{d\ln T} = H_v + V_l \frac{dP}{d\ln T}$$

and it will be assumed that the terms on the right hand side are constant over the temperature range utilized (95 to 105 ^oC). The values for these terms at 100 ^oC are

ΔH_v = 22259 cm^3 atm g^{-1} (cm^3 atm g^{-1} = 10^3 m^3 atm g^{-1} = 10^3 Nm g^{-1} = 10^3 J g^{-1})
V_l = 1.043 cm^3 g^{-1}
dP/dlnT = 13.33 atm

Therefore

$$V_g \frac{dP}{d\ln T} = 22272.9 \frac{cm^3 \text{ atm}}{g}$$

The specific volume of the water vapor is a function of temperature and pressure but deviations from ideal behavior would be expected so that the "gas constant" will be calculated from the thermodynamic properties of water at 100 ^oC. Assume that

$$V_g = R' \frac{T}{P}$$

so that

$$Vg \frac{dP}{d\ln T} = -R' \frac{d\ln P}{d\ 1/T} = 22272.9 \frac{(cm^3 \text{ atm})}{g}$$

or

$$R' = -22272.9 \frac{d\ 1/T}{d\ln P}$$

The average value of d (1/T)/dlnP over the temperature range 97 ^oC to 103 ^oC is $-2.016 \times 10^{-4} {}^oC^{-1}$ so that

$$R' = 4.4902 \frac{(cm^3 \text{ atm})}{g\ {}^oC}$$

Therefore

$$H_v = \frac{-V_1\, dP}{d\ln T} + \frac{R'\, T_1\, T_2}{T_2 - T_1} \ln\left(\frac{P_2}{P_1}\right)$$

or

$$H_v = -13.9 \frac{(cm^3\ atm)}{g} + 4.4902 \frac{(cm^3\ atm)}{g\ ^oC} \frac{T_1\, T_2}{T_2 - T_1} \ln\left(\frac{P_2}{P_1}\right)$$

Error Analysis

The probable error in the determination of H_v is given by

$$\Delta\Delta H_v = \frac{1669.8}{\ln T_1 - \ln T_2} \left[2\Delta p^2 + \frac{(P_1 - P_2)^2}{(\ln T_1 - \ln T_2)^2} (\Delta T)^2 \left(\frac{1}{T_1^2} + \frac{1}{T_2^2}\right)\right]^{\frac{1}{2}}$$

For the conditions

$P_1 = 1.192$ $T_1 = 378$ $\ln T_1 = .935$

$P_2 = 0.834$ $T_2 = 368$ $\ln T_2 = 5.908$

$$\Delta\Delta H_v = 61844[2\Delta P^2 + 25 \times 10^{-4} (\Delta T)^2]^{\frac{1}{2}}$$

If

$$\Delta T = 10^{-2}\ ^oC \text{ and } \Delta P = 10^{-4}\ atm$$

$$\Delta\Delta H_v = \pm 32 \frac{(cm^3\ atm)}{g}$$

The percent error is

$$\frac{\Delta\Delta H_v \times 100}{H_v} = \frac{3200}{22259} = 0.14\%$$

Effect of Gravity on Vapor Pressure of H_2O at 100°C

The effect of pressure on the vapor pressure of a fluid is given by

$$\ln\left(\frac{P}{P_o}\right) = \frac{V_1 P_e}{RT}$$

where P is the vapor pressure at a pressure P_e, P_o the vapor pressure at $P_e = 0$, V_1 the molar volume of liquid, R the gas constant, and T the temperature. In the present application, the vapor pressure of water is determined by the pressure at the water - water vapor interface, or the pressure on a mono-

layer of water due to a force field on one g, compared to zero g. For one gram mole of liquid water V_1 = 18 cm^3 and the area of the monolayer is

$$A = \left(\frac{18\ cm^3}{6 \times 10^{23}\ \text{molecules}}\right)^{2/3} (6 \times 10^{23}) = 5.8 \times 10^8\ cm^2$$

The pressure is $P = \frac{F}{A} = \frac{\bar{m}g}{A} = \frac{0.018 \times 9.8\ N}{5.8 \times 10^4\ m^2}$

$= 3 \times 10^{-6}$ Pa or 3×10^{-11} atm

Therefore

$$\ln\left(\frac{P}{P_o}\right) = \frac{18\ cm^3\ 3 \times 10^{-11}\ atm\ K}{373\ K\ 82\ cm^3\ atm} = 1.7 \times 10^{-14}\ K$$

From this, it is apparent that the difference in water vapor pressure and therefore boiling point between one g and zero g is negligible.

Component Specifications

Container

Volume 10 cm^3, to withstand internal pressure of 4 atm and external pressure of 2 atm.

Pressure Transducer

Pressure tolerance 0 to 2.2 atm, readability range 0 to 1.5 atm, accuracy + 0.0001 atm over 0.8 to 1.2 atm range.

Temperature sensor

Accuracy $\pm$ 0.05 °C, reproducibility $\pm$ 0.01 °C over 90 °C to 110 °C range.

Hardware Description

Experiment E, Zero Gravity Boiling Temperature and Latent Heat of Vaporization is shown in the Eu (unwicked) configuration in Figure 11. The experiment holds a sample of liquid water and water vapor in a sealed stainless steel container within a second container filled with water. In the Ew (wicked) configuration, the inner container is filled with water in a dacron wick. The outer container is insulated and is pressurized by a spring loaded bellows to prevent boiling when the water is heated by a temperature controlled resistance heating element wrapped around

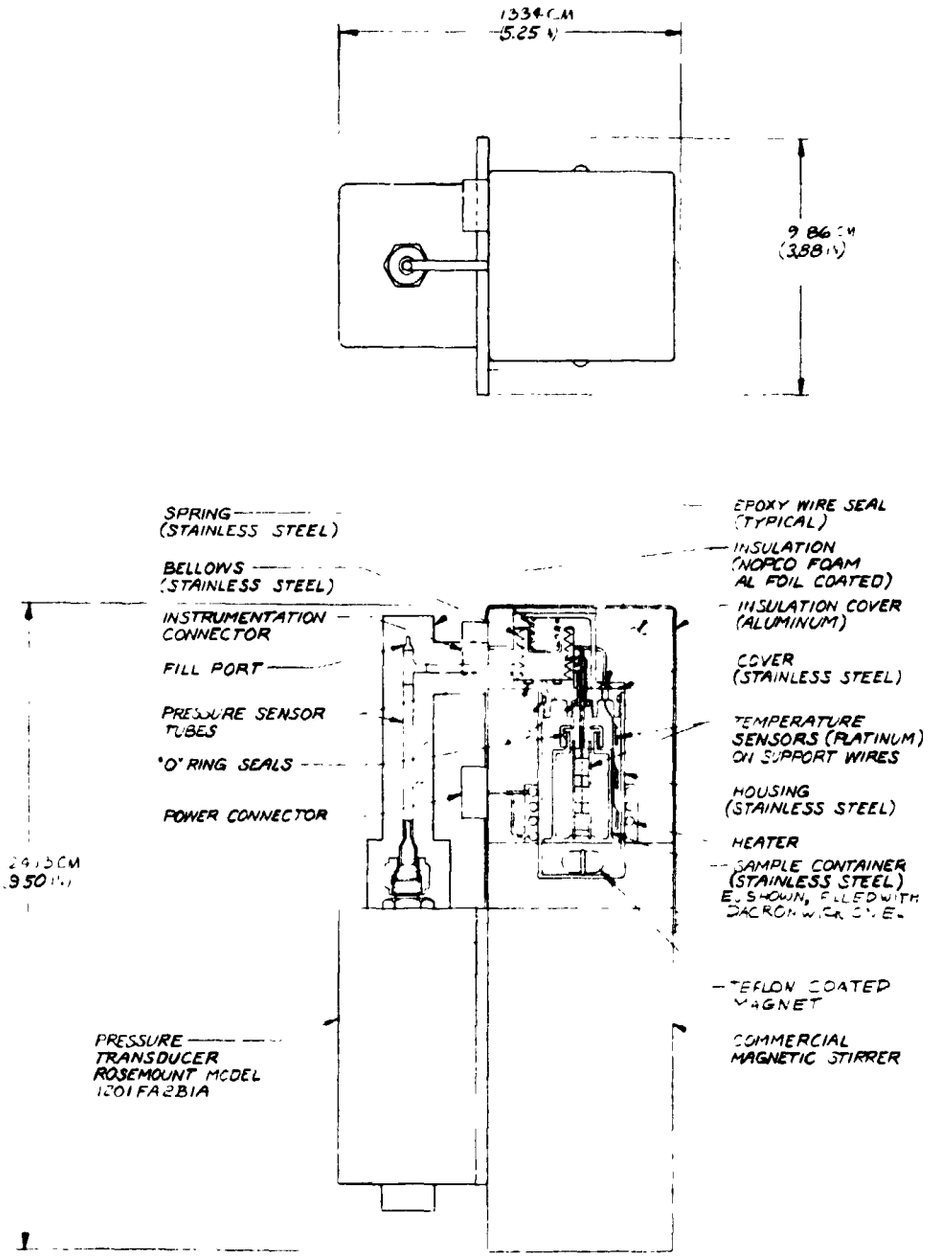

FIGURE 11

EXPERIMENT Eu AND Ew ZERO GRAVITY BOILING TEMPERATURE AND LATENT HEAT OF VAPORIZATION HARDWARE ARRANGEMENT

the container. A magnetic stirrer in the outer container assures uniform temperature distribution over the sample container. Both outer and inner containers have platinum resistance temperature sensing elements mounted on wire supports. The sensor wires in the sample container exit through a tube that connects to a Rosemont Model 1201FA2B1A Pressure Transducer. The wires are brought out through one leg of a Tee junction immediately outside the container. A second tee in this tube provides a crimped and sealed fill port. Insulation prevents heat loss from the containers and the tube.

Experiment Sequence

Experiments Eu and Ew are operated as follows:

a. Turn on temperature and pressure electronics and allow warm-up.

b. Turn on container heater and stirrer.

c. Control bath temperature at 95 ^{o}C $\pm$ 0.1 ^{o}C

d. Record sample pressure and temperature when sample and bath temperatures are equal within $\pm$ 0.02 ^{o}C.

e. Repeat c & d at 1 ^{o}C intervals increasing from 95 ^{o}C to 105 ^{o}C.

f. Repeat c & d at 1 ^{o}C intervals decreasing from 105 ^{o}C to 95 ^{o}C.

g. Turn off all equipment.

Appropriateness of Experiment

This experiment is intended to determine the change in boiling point of water in a zero gravity environment compared to a one gravity environment, and to determine the change in the latent heat of vaporization of water in a zero gravity environment compared to a one gravity environment. Analysis has shown that the change in water vapor pressure and, hence, the change in boiling temperature of water is negligible. No reasons exist to expect a significant change in the latent heat of vaporization of water, and experimental verification can be implied since performance durations vs. water usage of various zero gravity water boilers have been as expected. Therefore, it is concluded that this experiment must be treated as having only academic interest.

F-1. ZERO GRAVITY WICKING RATE

Objective

The objective of this module is to measure zero gravity wicking rate as a function of temperature difference where the driving force is due to interfacial tension.

Description of Experiment

A cell which is basically two square ducts in parallel and connected at the ends, as shown in figure 12, is used for this experiment. One of the ducts contains Dacron wick material and two platinum gauze electrodes. The cell is vacuum filled with distilled water containing a trace amount of electrolyte to give a stable zeta potential and insure a repeatable streaming potential. One end of the cell is maintained at a temperature T_2 and the other end at T_1 ($T_2 > T_1$). The resulting interfacial tension gradient will cause the water to flow around the loop and a streaming potential will be developed between the platinum gauze electrodes. A calibration curve relating the magnitude of the streaming potential to the water flow rate and pressure drop will be determined in a separate experiment on the Dacron wick material in the same solution.

Analytical Investigation

Flow Rate and Temperature

The cell can be considered as two square ducts of equal length in series with one duct containing the Dacron wick material as shown below.

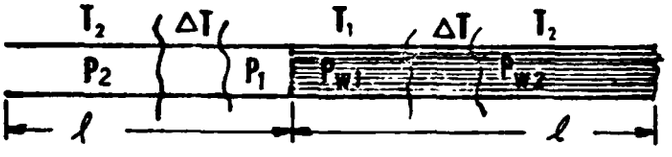

The pressure differences are given by

$$P_2 - P_1 = \frac{2 \cos \theta}{r} \frac{d\gamma}{dt} (T_2 - T_1) = \Delta P'$$

$$Pw_2 - Pw_1 = \frac{2 \cos \theta}{r_w} \frac{d\gamma}{dt} (T_2 - T_1) = \Delta Pw$$

Where r is the equivalent radius of the plain duct and r_w is the average capillary radius in the wick material. It is obvious that $r \gg r_w$ so that the magnitude of ΔP_w is greater than $\Delta P'$. The total pressure difference across the system is

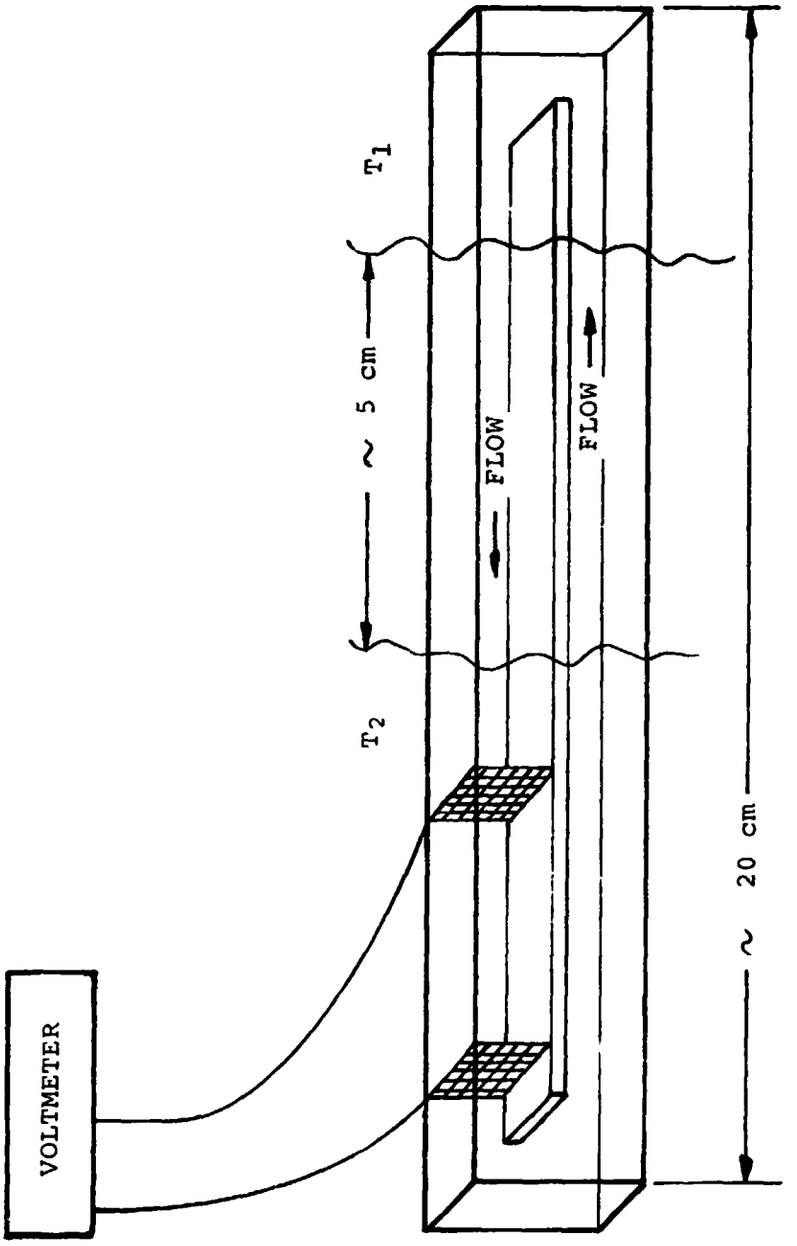

FIGURE 12: ZERO GRAVITY WICKING RATE MODULE

$$\Delta P = \Delta P_w - \Delta P' = \frac{2 \cos\theta \ d\gamma}{dt} (T_2 - T_1)\left[\frac{1}{r_w} - \frac{1}{r}\right]$$

the term $d\gamma/dt$ is negative (-1.645×10^{-4} kg s^{-2} $^{o}C^{-1}$) so that the direction of flow will be from T_1 to T_2 in the wick material.

Combining this equation with Poiseuille's equation gives

$$\frac{dV}{dt} = \frac{\pi \cos\theta}{4\eta\ell} \frac{d\gamma}{dt} (T_2 - T_1)\left[\frac{1}{r_w} - \frac{1}{r}\right]\left[\frac{nr_w^4 \ r^4}{nr_w^4 + r^4}\right]$$

where n is the number of capillaries in parallel and since $r \gg r_w$,

$$\frac{dV}{dt} = \frac{\pi \cos\theta}{4\eta\ell} \frac{d\gamma}{dt} (T_2 - T_1) \ nr_w^3$$

For the following values

$\eta = 10^{-3}$ kgs^{-1} m^{-1}
$\ell = 0.1$ m
$\cos\theta = 1$
$d\gamma/dt = -1.645 \times 10^{-4}$ kg s^{-2} $^{o}C^{-1}$
$(T_2 - T_1) = 10$ ^{o}C

$$dV/dt = -12.92 \ nr_w^3$$

The term r_w can be estimated for our wick material from liquid/vapor capillary rise experiments, e.g.

$$r_w = \frac{2\gamma\cos\theta}{gh}$$

and the n term can be calculated from a knowledge of the void volume of the wick material. Tentative values for n and r_w are 3×10^3 and 10^{-2} cm, respectively, which gives a volume flow rate of -2 cm^3 per minute.

Streaming Potential*

The streaming potential is given by

$$E_s = \frac{D\zeta \cos\theta}{2\pi\eta\lambda r_w} \frac{d\gamma}{dt} (T_2 - T_1)$$

With the following values

*Davies, J. T. and Rideal, E. K., "Interfacial Phenomena", Academic Press, New York, 1961.

$\zeta = 5 \times 10^{-2} V$ (typical value)

$\cos\theta = 1$

$d\gamma/dt = -1.645 \times 10^{-4}$ kg s^{-2} $^{o}C^{-1}$

$(T_2 - T_1) = 10\ ^{o}C$

$D = 8/9 \times 10^{-8}\ A^2\ s^4\ kg^{-1}\ m^{-3}$

$\eta = 10^{-3}$ kg s-1 m^{-1}

$\lambda = 10^{-6}$ ohm^{-1} $cm^{-1} = 10^{-4}$ kg^{-1} m^{-3} s^3 A^2

$r_w = 10^{-2}$ cm $= 10^{-4}$ m

$E_s = -11.6$ mV

The value of the streaming potential will be directly proportional to (T_2-T_1) or ΔP and inversely proportional to the average capillary radius r_w. The value of r_w (10^{-2} cm) is felt to be on the high side so that larger values for the streaming potential (assuming the typical 50 mV zeta potential) may be expected.

Heat Transfer Rate

The conductive heat transfer rate for a 10 ^{o}C temperature differential over a 5 cm distance is given by

$$\bar{W} = \frac{6.28\ mW\ A}{cm\ ^{o}C} \quad \frac{(T_2-T_1)}{\Delta X}$$

for $A = 2 \times 1.44\ cm^2$

$\bar{W} = 36.2$ mW

The convective heat transfer rate for a 2 g per minute water flow rate will be

$$\bar{W} = mCp\ (T_2-T_1) = \frac{2\ g}{min} \quad \frac{4.187\ J}{g\ ^{o}C} \quad \frac{10\ ^{o}C\ min}{60\ s} = 1.4\ W$$

The mass flow rate of the heat transfer fluid necessary to maintain T_2 and T_1 uniform to $\pm 0.5^{o}C$ and remove heat at the rate of 2 W is

$$m = \frac{\bar{W}}{Cp\ (T_2-T_1)} = \frac{2\ Jg \qquad ^{o}C\ 60s}{4.197\ Js\ 0.5\ ^{o}C\ min} = \frac{57.3\ g}{min}$$

Component Specifications

Cell Dimensions

1.2 cm x 1.2 cm x 20 cm long. Insulated temperature differential path length 5 cm.

Cell Material

Must be electrical insulator.

Electrodes

52 mesh screen, platinum 5 to 10% rhodium or iridium, 4 cm separation.

Voltage Measurement

$>10^{12}$ ohms input resistance, readable to $\pm$0.1 mV.

Heat Transfer Fluid

Temperature controlled to $\pm$0.1 ^{o}C, flow rate 100 g/min.

Hardware Description

Experiment F-1, Zero Gravity Wicking Rate, shown in Figure 13, consists of a teflon housing containing two rectangular passages connected at each end. One of these passages is filled with water saturated dacron wick material, the other is filled with bulk water. The passages are separated by a "U"shaped teflon wick support. The wick material contains two platinum screen electrodes and three platinum resistance temperature sensing elements. The wick, support, and water sample is sealed by an elastomeric "O" seal and an insulated stainless steel backed teflon cover. A 5 cm section in the center of the housing is also insulated. Each end of the remainder of the housing is constructed to surround three sides and the end of the sample with a heat exchanging water jacket that can conduct heat through the thin teflon wall to the water sample. This thin wall area also flexes to allow for sample volume thermal expansion. These water jackets are sealed by a single stainless upper housing bolted against two rectangular face type "O" seal grooves in the telfon housing. The bolts extend through the housing to retain the insulated cover over the sample chamber. The upper housing contains inlet and outlet ports as well as a cavity for a special spiral finned resistance heating element. A common latching solenoid valve is attached to bosses on the side of the upper housing.

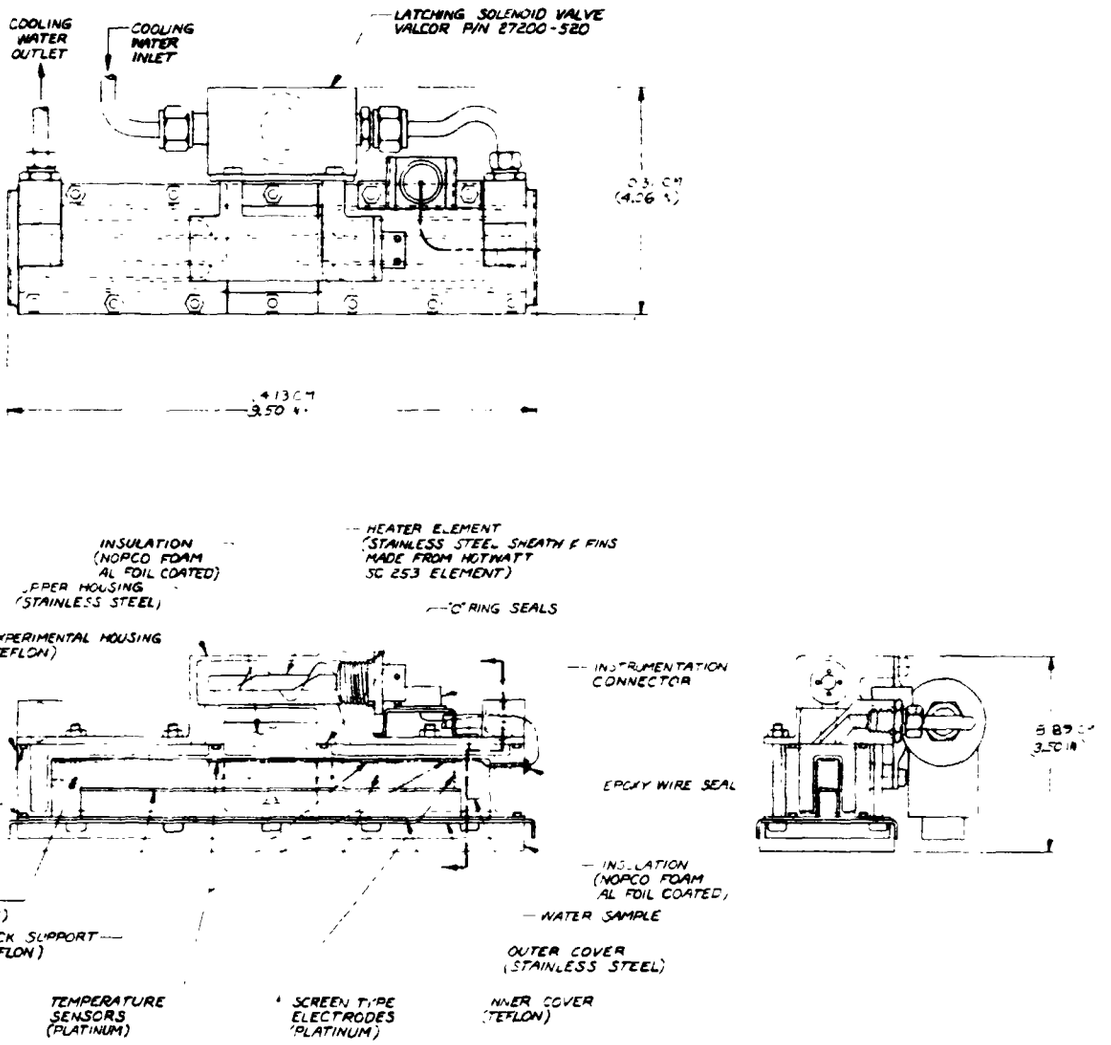

FIGURE 13 EXPERIMENT F-1 ZERO GRAVITY WICKING RATE HARDWARE ARRANGEMENT

Experiment Sequence

Experiment F-1 is operated as follows:

a. Open water valve.

b. Turn on temperature sensors and heater.

c. Turn on temperature control to 5 ^{o}C temperature differential setting.

d. Allow 10 minute stabilization period.

e. Record voltage and temperatures at electrodes every minute for 10 minutes.

f. Repeat c, d, and e for a 10 ^{o}C temperature differential setting and again for 15^{o}C temperature differential.

g. Turn off equipment.

Appropriateness of Experiment

This experiment is intended to demonstrate and measure zero gravity wicking rate as a function of temperature difference. A thorough examination of available literature has failed to turn up background material indicating that any effort has been expended in the area where no liquid/vapor interface exists and, therefore, a significant scientific advancement can be achieved by demonstrating and measuring this wicking rate. A one gravity version of this experiment can be constructed to verify the existence of the driving force.

F-2. ZERO GRAVITY WICK WETTING CHARACTERISTICS

Objective

The objective of this module is to determine the wetting characteristics of a Dacron wick material.

Description of Experiment

A cell consisting of two long parallel metal plates with Dacron wick material between the plates will be used to conduct this experiment. One end of the cell is connected to a water reservoir with a shut-off valve and the other end is opened to ambient. When the valve is opened, the wicking rate is determined by measuring the cell capacitance as a function of time.

Analytical Investigation

The cell capacitance is given by:

$$C = \Sigma \epsilon_o D \frac{a}{d} = \epsilon_o \frac{a}{d} [D_c (L-\ell) + D_w \ell]$$

where ϵ_o is the permissivity (8.8542×10^{-12} C^2 N^{-1} m^{-2}), a the width, d the thickness, L the total length, ℓ the wetted length, and D the dielectric constant. Assuming the following values:

$a = 2 \times 10^{-2}$ m
$d = 4 \times 10^{-3}$ m
$L = 2 \times 10^{-1}$ m
$D_c = 2$ (dry wick)
$D_w = 80$ (wet wick)

Rearranging the cell capacitance equation for ℓ:

$$\ell = \frac{dC}{a \epsilon_o (D_w - D_c)} - \frac{D_c L}{D_w - D_c}$$

$$\ell = 2.9 \times 10^8 \, C - 5.13 \times 10^{-3}$$

where ℓ is in meters and C in farads. Thus the capacitance will vary from 17.7 pF at $\ell = 0$ to 708 pF at $\ell = L$ (0.2 m).

The time required for the wick to fill completely with water ($\ell = L$) is given by

$$t = \frac{2\eta L^2}{\gamma r_w \cos\theta}$$ Rideal-Washburn Equation*

Assuming:

$\eta = 10^{-3}$ kg m^{-1} s^{-1}
L = 0.2 m
$\gamma = 7.2 \times 10^{-2}$ kg s^{-2}
$r_w = 10^{-4}$ m
$\cos\theta = 1$

t = 11.1 s

Since the value for r_w (10^{-4} m) is believed to be high, the actual time for complete filling of the wick should be greater than 11 seconds.

Component Specifications

Cell

Internal dimensions, 0.4 cm thick, 2 cm wide, 20 cm long, metal plates - rhodium plated copper.

Reservoir Volume

20 cm^3

Capacitance Measurement

Range 15 pF to 800 pF, reproducibility ± 1 pF, one reading per second.

*Davies, J. T. and Rideal, E. K., "Interfacial Phenomena", Academic Press, New York, 1961.

Hardware Description

Experiment F-2, Zero Gravity Wick Wetting Characteristis, shown in figure 14, holds a sample of dacron wick material between two rhodium plated copper plates that are held apart by separators of teflon. These plates are wired to act as capacitive elements for measurements of wick liquid content and are covered with a thin walled rubber tube that acts as insulation. This assembly is bonded into, and insulated from, an aluminum housing that contains the experiment water sample. The water is prevented from entering the wick by a silicone rubber seal attached to the end of a spring loaded hinged link. A solenoid attached to the housing is activated to lift the seal from the end of the wick to expose the wick to the water reservoir. A silicone rubber diaphragm supported by a perforated aluminum plate contains the water sample within the housing, and flexes to allow unrestricted flow of water into the wick. Since Experiment F-2 is a non-repeatable experiment, three modules are included in the overall experiment to verify experimental repeatability.

Experiment Sequence

Experiment F-2 is operated as follows:

a. Activate capacitance circuit and index controller to module F-2a.

b. Energize solenoid and start timer.

c. Record capacitance and time at ten second intervals for 10 minutes.

d. Index controller to module F-2b and repeat steps b and c.

e. Index controller to module F-2c and repeat steps b and c.

f. Turn off equipment.

Appropriateness of Experiment

This experiment is intended to measure wetting characteristics of dacron wick material. A similar experiment was attempted unsuccessfully during the Skylab experimentation. Due to the fact that this phenomenon can be studied adequately in a one gravity environment it must be concluded that the experiment is unnecessary.

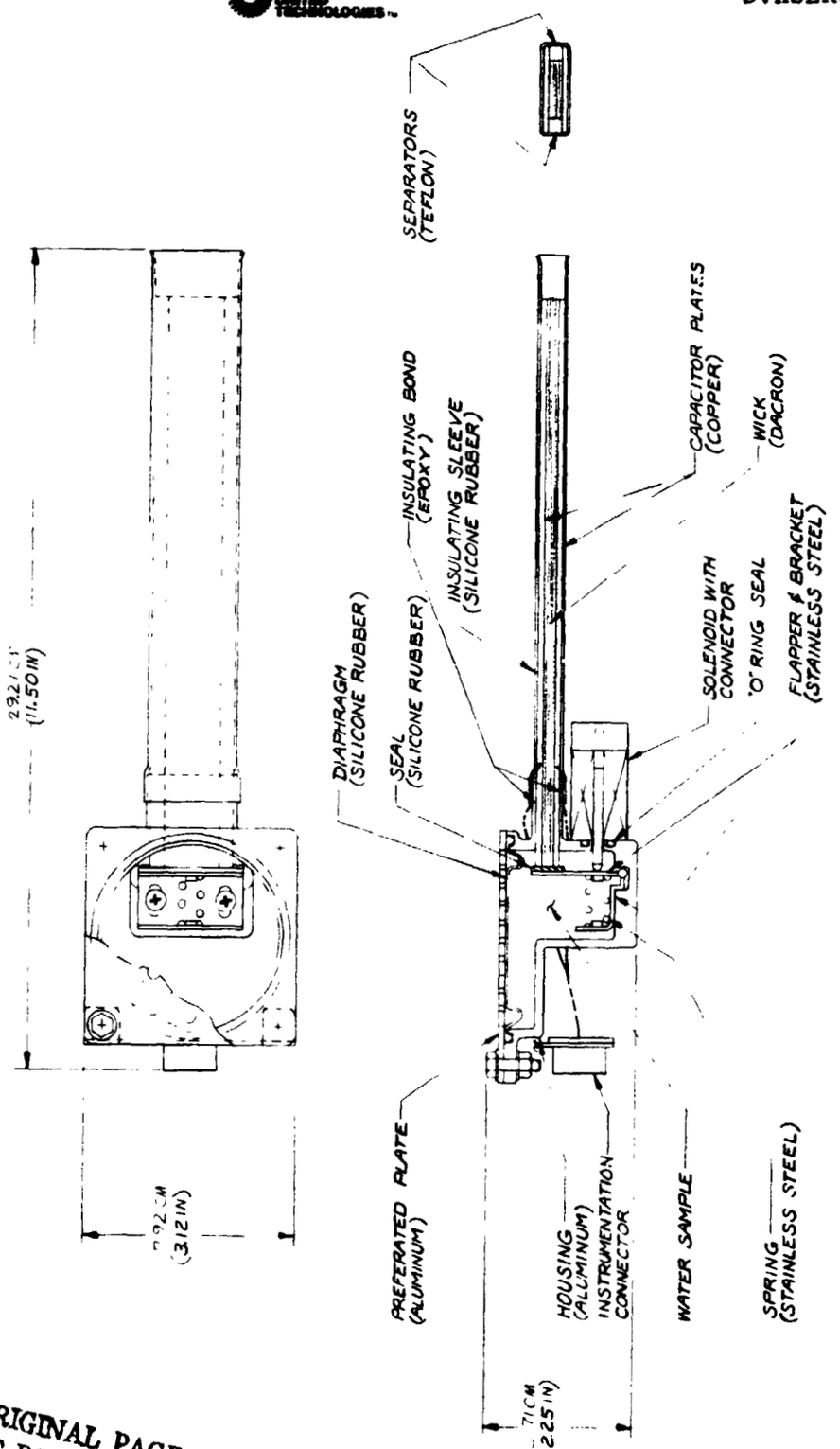

FIGURE 14

EXPERIMENT F-2 ZERO GRAVITY WICK WETTING CHARACTERISTICS
HARDWARE ARRANGEMENT

F-3 ZERO GRAVITY WICK DRYOUT CHARACTERISTICS

Objective

The objective of this experiment is to determine the dryout characteristics of dacron wick material.

Description of Experiment

The basic cell for this experiment contains a 4mm thick plate wrapped with a single layer of dacron wick material such that the wick material covers both sides of the plate and one short end. This end is compressed against a heated perforated metal evaporator plate. Perforations in the evaporator expose the wick to a low pressure cavity which in turn is exposed to vacuum via a downstream choking orifice. A Neucleonics radiation source is placed on one side of the cell and five radiation detectors on the other side.

The wick material is initially completely filled with distilled water. The experiment is started by opening a vacuum valve and supplying heat to the evaporator plate to maintain a constant temperature (ambient) in the evaporation zone. As the water evaporates from the end of the cell any maldistribution of water within the wick will be detected from variations in the radiation level passing through the cell.

Analytical Investigation

Cell volume = 4 cm x 23 cm x 0.8 cm = 73.6 cm^3

Void volume = 0.835 x 73.6 = 61.4 cm^3

Heat required for evaporation at 20 °C

$$2450 \frac{J}{g} \times 61.4\ g = 150.4\ kJ$$

Time for complete evaporation

Assume 4 W input to evaporation plate

$$\frac{150.4\ kJ\ s\ hr}{4\ J\ 3600\ s} = 10.4\ hrs$$

Choking Orifice

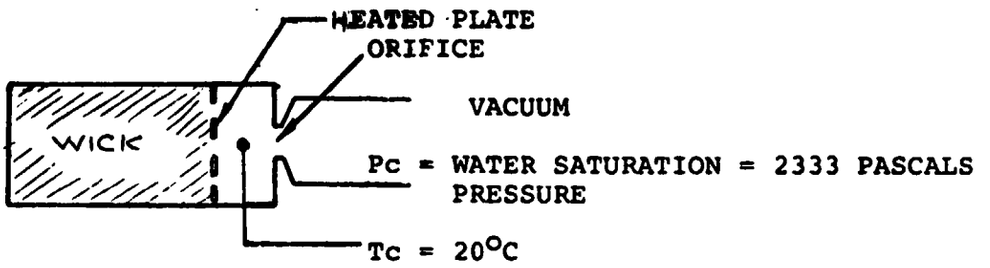

γ Water = 1.244
@20°C

Required Mass-Flow

$$\dot{m} = \frac{0.061 \text{ kg}}{10.4 \text{ hr}} = 5.865 \times 10^{-3} \frac{\text{kg}}{\text{hr}}$$

$$\dot{m} = 1.629 \times 10^{-6} \frac{\text{kg}}{\text{sec}}$$

$$\dot{m} \text{ (Choked Flow)} = C_D A_t P_c \left[\frac{\gamma}{R} \left(\frac{2}{\gamma+1} \right)^{\frac{\gamma+1}{\gamma-1}} \frac{M_w}{T_c} \right]^{\frac{1}{2}}$$

& Since $A_t = \frac{\pi (d^*)^2}{4}$

$$(d^*)^2 = \frac{4}{\pi} \frac{\dot{m}}{C_D P_c \left[\frac{\gamma}{R} \left(\frac{2}{\gamma+1} \right)^{\frac{\gamma+1}{\gamma-1}} \frac{M_w}{T_c} \right]^{\frac{1}{2}}}$$

Let $\Gamma = \left[\gamma \left(\frac{2}{\gamma+1} \right)^{\frac{\gamma+1}{\gamma-1}} \right]^{\frac{1}{2}}$

then $(d^*)^2 = \dfrac{4 \dot{m}}{\pi C_D P_c \Gamma \left(\frac{M_w}{RT_c} \right)^{\frac{1}{2}}}$

where: $\dot{m} = 1.629 \times 10^{-6}$ kg sec^{-1}
$T_c = 293$ K
$P_c = 2333$ Pa
$M_w = 18$ kg kmole^{-1}
$R = 8.314 \times 10^3$ J kmole^{-1} K^{-1}
$\Gamma = 0.6569$
$C_D = 0.6$ (Discharge coef. for sharp-edge orifice)
$\gamma = 1.244$

$$(d^*)^2 = \frac{(4)\ (1.629 \times 10^{-6})}{\pi\ (.6)\ \ (2333)\ \ (.6569)\ \left[\frac{18}{(8.314 \times 10^3)\ (293)} \right]^{\frac{1}{2}}}$$

$(d^*)^2 = 8.298 \times 10^{-7}$ m^2

$d^* = 9.109 \times 10^{-4}$ m

Component Specifications

Cell Internal Dimensions

1.2 cm x 4 cm x 23 cm

Center Plate Dimensions

0.4 cm x 4 cm x 20.5 cm

Heat Input to Evaporator Plate

4 W nominal, 6 W maximum

Orifice Size

0.9109 mm

Hardware Description

Experiment F-3, Zero Gravity Wick Dryout Characteristics, shown in figure 15, utilizes an all teflon housing to contain a dacron wick sample folded into a "U" shape over a teflon strip. The strip is used to compress the closed end of the "U" against an aluminum end block which encloses one end of the housing. A teflon end plate seals the other end of the housing and backs up the wick compressor strip. Holes are drilled in the end block to connect the wick area to a common outlet port which in turn is connected through a latching solenoid valve to a vacuum vent line. A silicone rubber enclosed resistance heating element is bonded to the exterior of the end block and covered with insulation. A platinum resistance temperature sensor is bonded to the inside of the end block and acts to control the temperature of the block. Since experiment F-3 is non-repeatable, three modules are included to verify experimental repeatability.

A nucleonics quantity sensor system is used to determine the amount and location of water in the wick of each module during the dryout experiment. Two radioactive General Nucleonics sources, P/N 1010-00-300-1, provide a safe, low level radiation field for all three modules. The sources are mounted to one of the modules with the other two modules arranged to form a triangle with the sources in the center. Each module has five General Nucleonics, P/N 1010-00-400-1, detector assemblies attached at equal intervals on the far side of the wick housing to detect the variable attenuation of the radiation level caused by local water quantity variation.

Experiment Sequence

Experiment F-3 is operated as follows:

a. Index controller to module F-3a.

b. Activate heater and temperature control.

c. Activate nucleonics detector elements.

d. Open vacuum valve and start timer.

e. Record quantity at all 5 detectors initially and at 10 minute intervals for ten hours.

HAMILTON STANDARD Division of UNITED TECHNOLOGIES

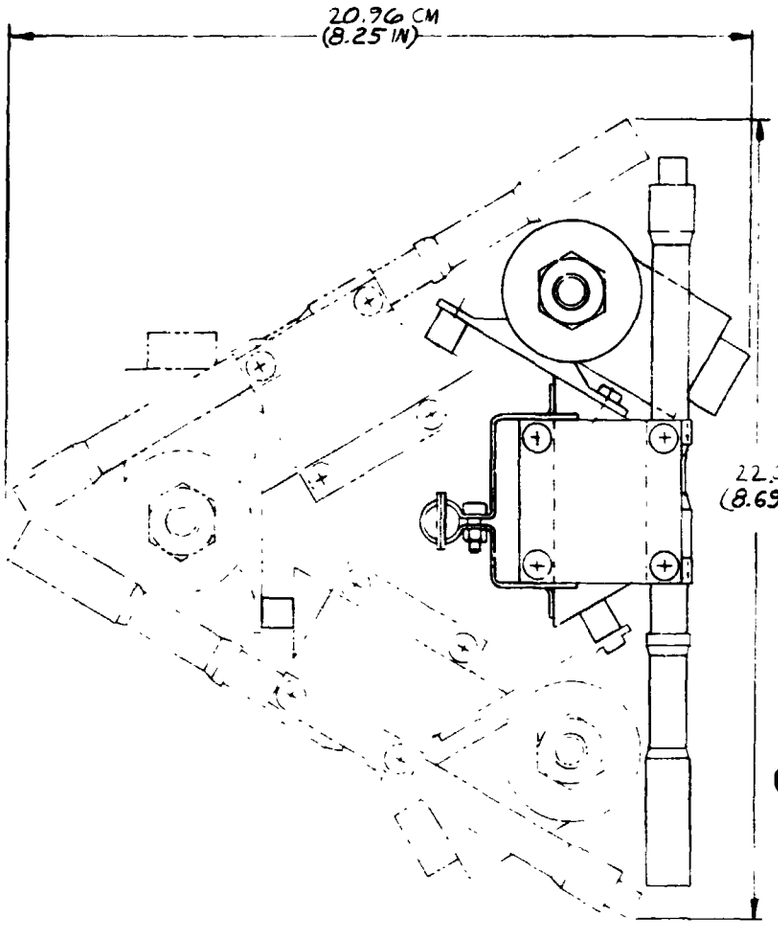

ARRANGEMENT OF 3 F_3 EXPERIMENTS SHARING COMMON SOURCE

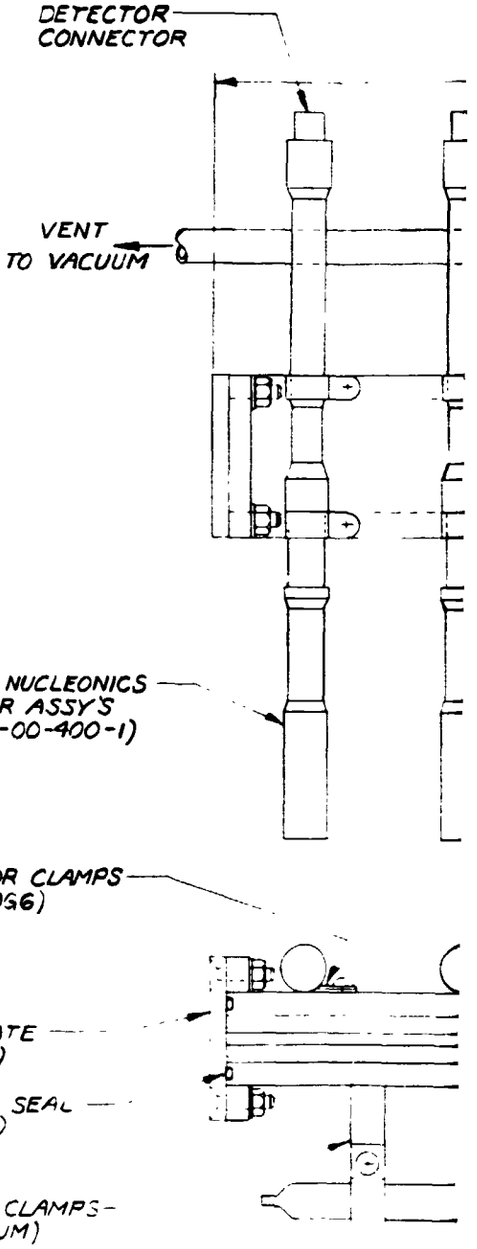

FOLDOUT FRAME /

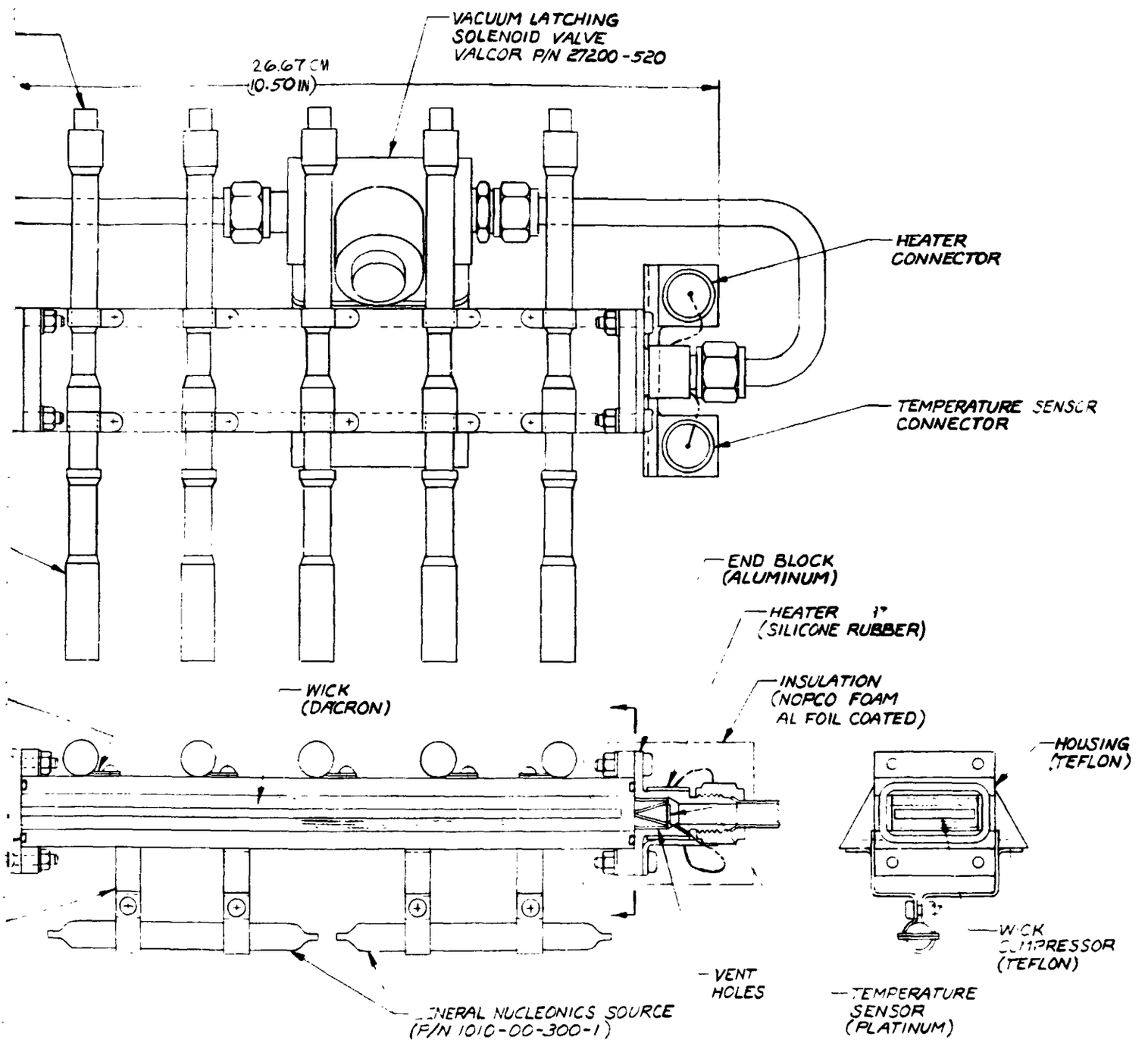

FIGURE 15:

EXPERIMENT F-3 ZERO GRAVITY
WICK DRYOUT CHARACTERISTICS
HARDWARE ARRANGEMENT

f. Index controller to module F-3b and repeat steps b thru e.

g. Index controller to module F-3c and repeat steps b thru e.

h. Turn off equipment.

Appropriateness of Experiment

This experiment is intended to determine wick dryout characteristics. It is speculated that a wick dries out in a sequence where the largest pores in the material (lowest surface tension) empty first and the smallest pores empty last. Due to the effect of the gravity field operating against the surface tension it is not possible to obtain an absolute assessment of this effect in one gravity. The performance of wetted wicks in zero gravity is extremely important in devices that utilize evaporative cooling. Therefore it is concluded that a significant engineering advancement can be achieved by determining zero gravity wick dryout characteristics.

PHENOMENA INTEGRATION

Objective

The Physical Phenomena Experiment Chest Concept integration has been carried out with the objectives of providing a simple to operate experiment package that will interface with the Spacelab pressurized cabin for the zero-gravity portion of the experiment, yet will allow one "g" check out of the experiment for calibration prior to flight. Each of the experiments previously described is controlled by electronic circuitry as part of the experiment package, and interfaces with vehicle services as required.

System Description

Figure 16 shows the electrical and mechanical relationship of the phenomena experiments to one another, and to the electronic boxes that control the experiments. Schematically the experiments are broken down into two groups. Group 1 contains A, C, and D; and Group 2 contains experiment B, E, F-1, F-2, and F-3. The inefficiency of the thermoelectric cooling devices, used in Experiments A, B, and C, and the high power required particularly in experiment A, influenced the grouping of the control function of these three experiments into one electronic control box which is configured to dissipate the heat of solid state switching of these high current devices to a cold plate connected to the cooling loop. The second control box handles the remaining experiments (B, E, F-1, F-2, and F-3). Each control box performs switching, power supply, and signal conditioning functions. A single processor box performs sequencing of actions in each experiment, and temporary storage of data prior to transmittal to the vehicle data acquisition system. The processor box is connected to both control boxes.

The experiments and the control boxes have specific interfaces with the vehicle to provide cooling, power, and other functions. These interfaces are defined in Table II.

HAMILTON STANDARD Division of UNITED TECHNOLOGIES

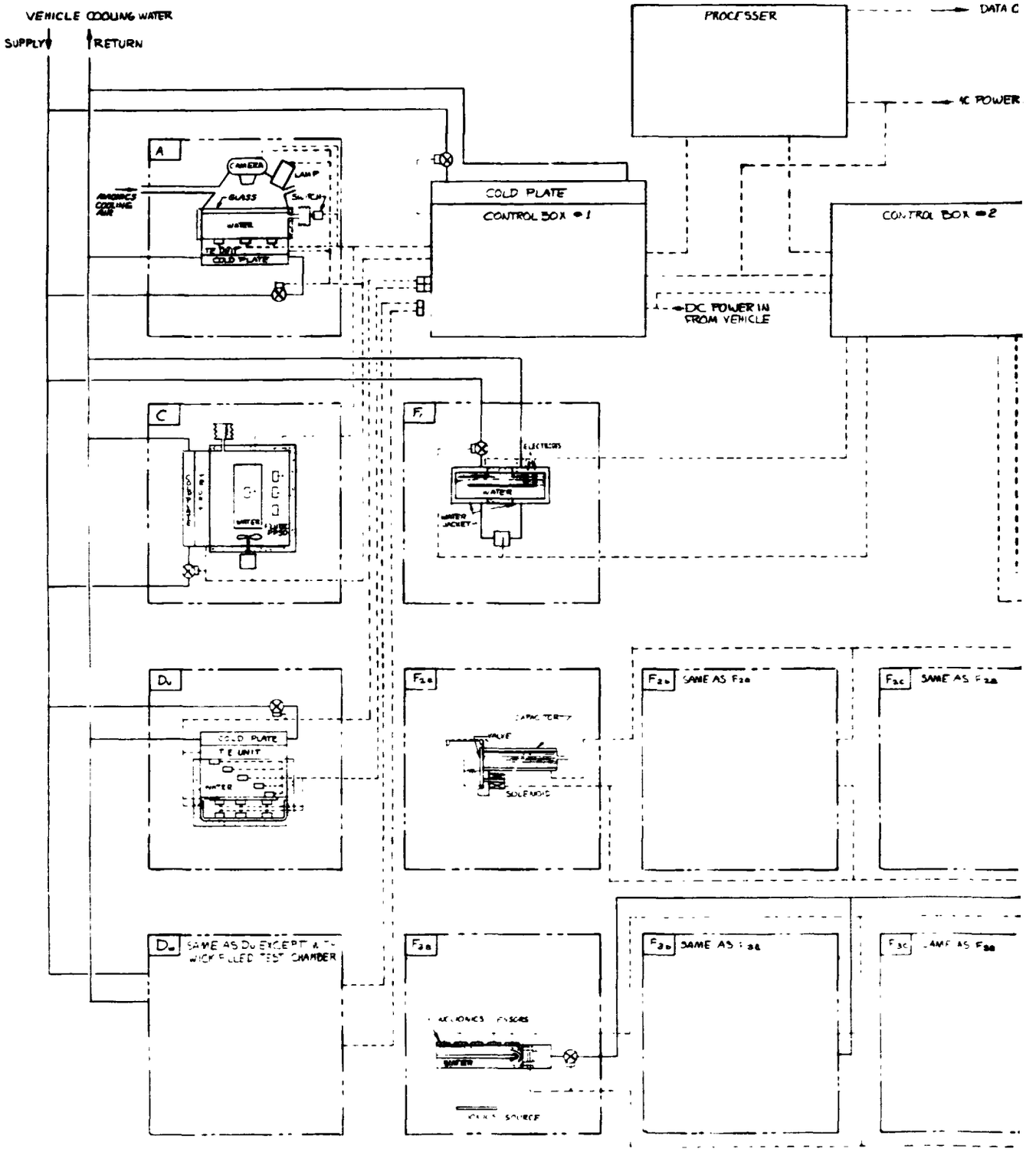

FOLDOUT FRAME 1

ORIGINAL PAGE IS
POOR QUALITY

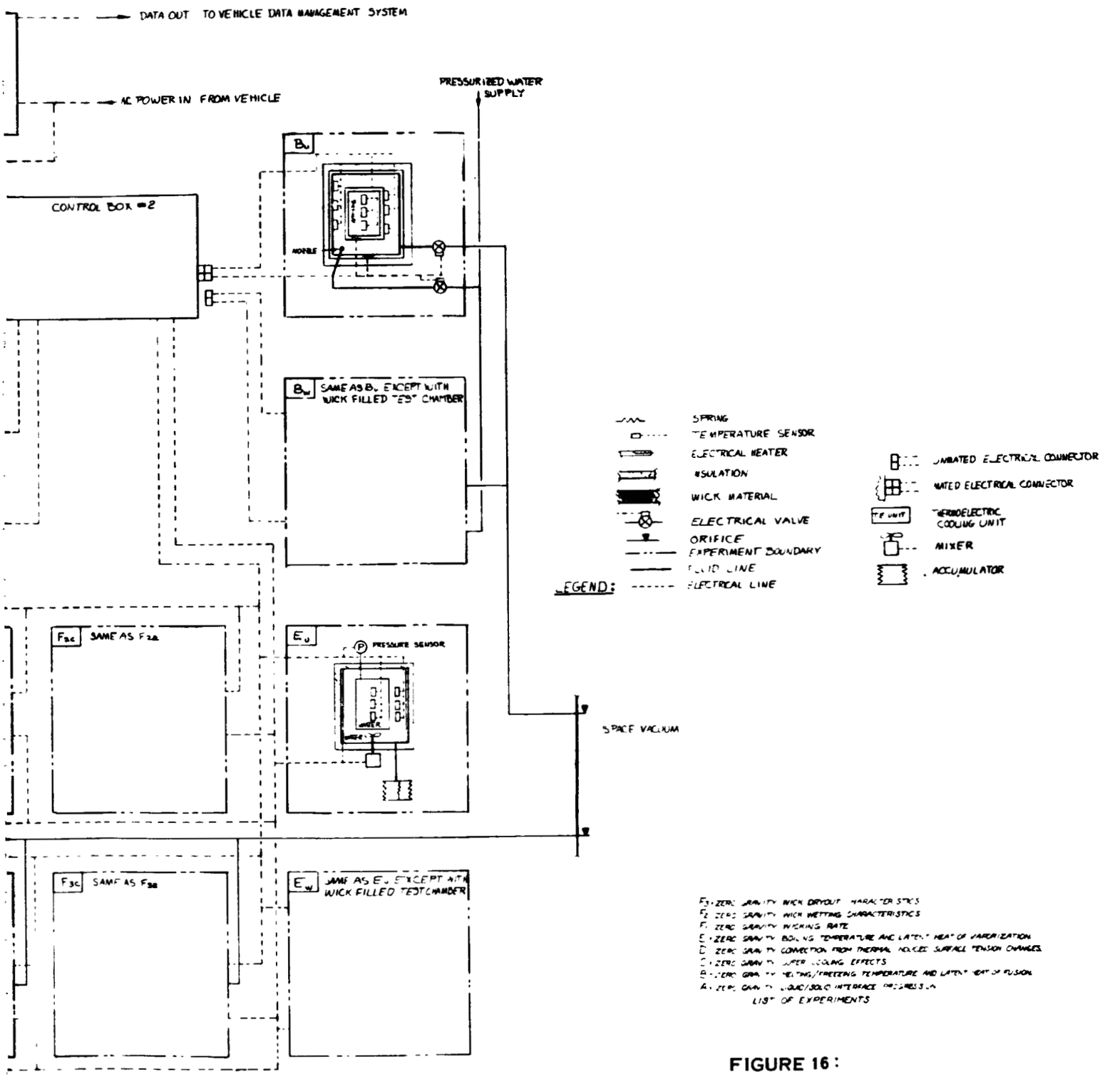

F_3: ZERO GRAVITY WICK DRYOUT CHARACTERISTICS
F_2: ZERO GRAVITY WICK WETTING CHARACTERISTICS
F_1: ZERO GRAVITY WICKING RATE
E: ZERO GRAVITY BOILING TEMPERATURE AND LATENT HEAT OF VAPORIZATION
D: ZERO GRAVITY CONVECTION FROM THERMAL AND/OR SURFACE TENSION CHANGES
C: ZERO GRAVITY SUPER COOLING EFFECTS
B: ZERO GRAVITY MELTING/FREEZING TEMPERATURE AND LATENT HEAT OF FUSION
A: ZERO GRAVITY LIQUID/SOLID INTERFACE PHENOMENA
LIST OF EXPERIMENTS

FIGURE 16:
PHYSICAL PHENOMENA EXPERIMENT CHEST BLOCK DIAGRAM

FOLDOUT FRAME 2

Vehicle Interface	Experiments								Box 1	Box 2	Processor
	A	B	C	D	E	F-1	F-2	F-3			
Cooling Water Loop	x		x	x		x			x		
Avionics Cooling Air	x										
Water Supply		x									
Space Vacuum Line		x						x			
AC Power									x	x	x
DC Power									x	x	

TABLE II VEHICLE INTERFACES

Electrical Control Configuration

Figure 17 shows the electrical block diagram for the ice pack experiment. All experiments require electrical process control with time-sequenced and/or level dependent commands. In addition, data from each experiment must be collected, stored temporarily, and transmitted to the on-board data acquisition system for permanent storage and eventual retrieval.

These requirements are satisfied by an electronic processor of the "Microprocessor" family. Electronics of this type are capable of providing multiple commands as a function of an internal program (stored in memory) to any or all of the experiment hardware simultaneously. Internal timing is provided by clock circuitry to generate time delays and intervals. In addition, the devices are programmed to respond to external instrumentation signals, e.g., comparing a sensor output to a pre-programmed reference and taking appropriate action.

The "processor" communicates with the individual experiments via two control boxes.

Electrical Hardware Description

The three electrical components are enclosed in aluminum boxes with environment and EMI sealing provisions. The electronics is nearly 100% solid state. Electromechanical relays will be considered for use where a significant weight or cost reduction can be achieved.

The processor unit contains a power supply to provide secondary supply voltages to operate the control circuitry and the processor itself. Since this power supply is essential for all experiments, it is redundant and fused individually for each experiment.

Main power in the form of single-phase 400 Hz, 115 VAC and 28 VDC will be used. The AC power is required primarily for the low power thermoelectric coolers to minimize current and efficiently provide conversion to the low voltage high current load drawn by these elements. DC power is used directly for the high power thermoelectric coolers in experiment A.

The control boxes contain the following types of circuits:

Solid state drive circuits for solenoid valves

Regulated voltage supplies for heaters

HAMILTON STANDARD Division of UNITED TECHNOLOGIES

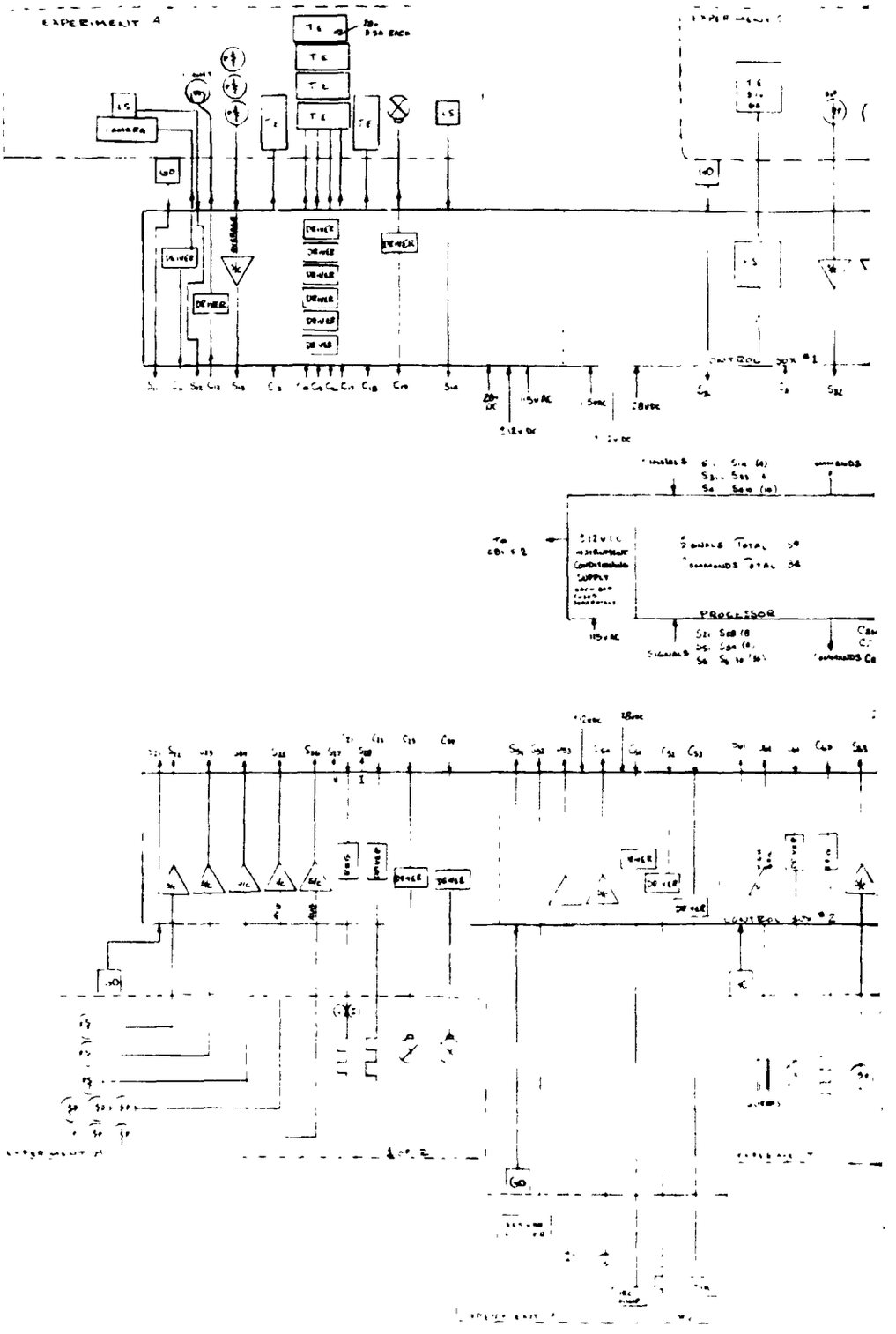

FOLDOUT FRAME 1

ORIGINAL PAGE IS
OF POOR QUALITY

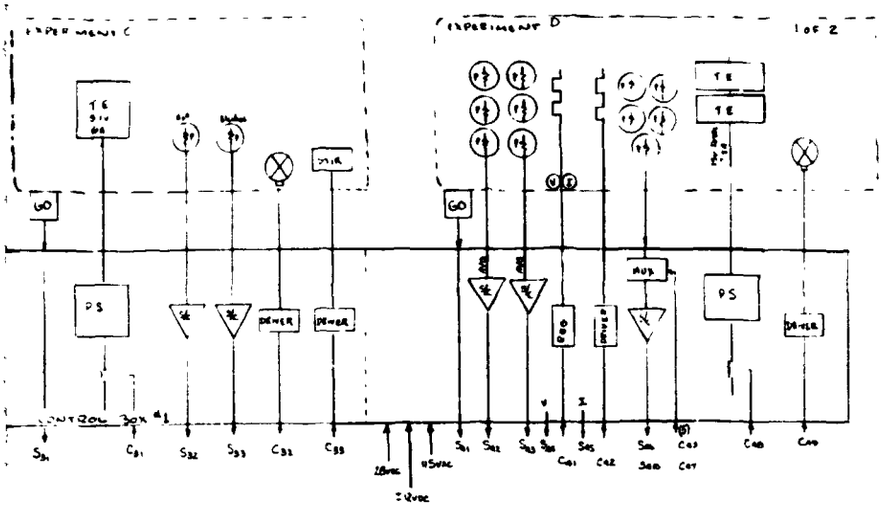

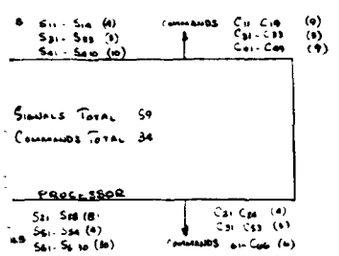

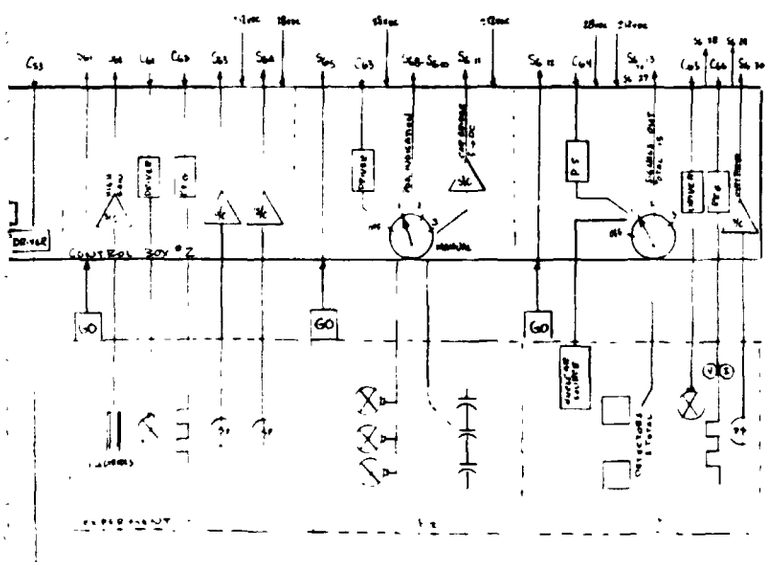

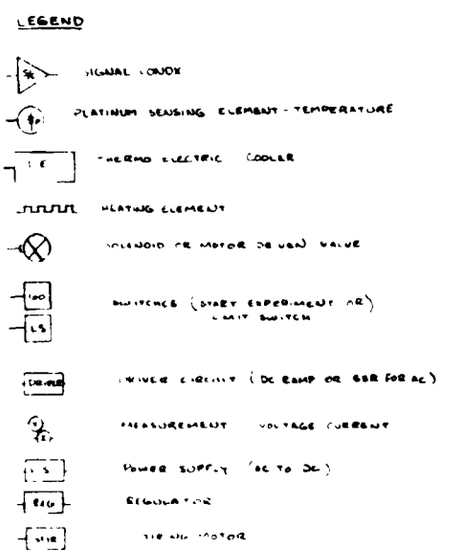

FIGURE 17:
PHYSICAL PHENOMENA EXPERIMENT CHEST
ELECTRICAL SCHEMATIC

FOLDOUT FRAME 2

Power supplies for thermoelectric coolers as required

Switch circuitry and electromechanical relays for on/off controls

Signal conditioning for instruments, primarily temperature sensors

Multiplex control circuitry

The electrical processing components for experiment Bu is identical to that required for Bw. Similarly Du equipment is identical to that required in Dw. In these experiments, platinum resistance temperature sensing elements are used in large numbers. Switching from Bu to Bw, or Du to Dw is desirable to utilize common components. Since contact resistance variations in mechanical switches could affect the sensor readings, the switching function is performed by manually disconnecting one experiment harness connector and connecting the other experiment harness connector to switch between the wicked and unwicked versions of these two experiments. The resulting resistance variation is negligible due to the intimate contact available in the electrical connectors.

Experiment Operation

Operation of a typical experiment is shown below using Experiment D as an example.

a. With experiment Du connected to control Box 1, start experiment with "GO" manual switch on processor box.

b. Equipment warmup period for suitable time programmed into processor.

c. Initial temperatures are sampled at end of warmup period for all sensors.

   1. Arithmetic average of 3 constant-power heater sensors.

   2. Arithmetic average of 3 ΔT sensors.

   3. Other sensors are multiplexed.

   All data stored in processor temporarily.

d. Thermo-electric units, cooling water valve, and constant-power heater are energized by processor command through driver circuits in control box. Voltage and

current of heater are sensed and data stored.

e. Voltage is applied to temperature control heater in such a manner as to maintain zero temperature differential. On/off control function is provided by the processor.

f. The temperature data from each sensor is conditioned and sampled by the processor every minute for one hour.

g. After one hour, all elements are de-energized.

h. Stored data is transmitted to the on-board data acquisition system in proper format on command.

i. Manual disconnect of Du, and connection of Dw prepares controller for operation of wicked configuration.

j. Repeat steps (a.) thru (h.) for experiment Dw.

Data Management

All of the information generated by the experiments that will be used for evaluation of the investigated phenomena is stored in the processor as it is generated by the individual experiments. On command from the vehicle data management system this information is transfered for recording and storage on board, or for transmittal to earth for ground evaluation while the flight is still in progress. This last procedure allows time to rerun certain experiments if desired.

Most of the stored information is in the form of temperature versus time data. However, some pressure, voltage capacitance, and quantity verses temperature data, and photographic film data also is collected and stored as shown in Table III. All information except the photographic film is stored in the processor memory banks as binary data bits representing voltages from the various sensor signal conditioning units.

Experiment	Type of Data	Data Points	Where Stored
A.	Photographic film exposure	30 per run	Camera
B.	Temperature versus time data	120 per run	Processor
C.	Temperature versus time data	60 per run	Processor
D.	Temperature versus time data	300 per run	Processor
E.	Temperature versus pressure data	20 per run	Processor
F.	Voltage verses time data temperature versus time data	33 per run 33 per run	Processor Processor
F2a,b,&c	Capacitance versus time	33 total	Processor
F3a,b,&c	Quantity versus time	33 total	Processor

TABLE III PHENOMENA DATA STORAGE

Phenomena Experiment Packaging

The selected packaging concept for the Physical Phenomena Experiment Chest is shown in Figure 18. It contains all experiment modules, and the three electrical control boxes within a structural framework of welded square aluminum tubing. The package configuration is designed to occupy the overhead portion of a Space Lab experiment rack which is a rectangular volume 800 mm X 550 mm x 572 mm. The Spacelab is the likely vehicle for this experiment since the vehicle and the Space Lab can be made operational at the same time. The Space Lab experiment rack location imposes the type of vehicle constraints and interface requirements that will be encountered when integrating a zero gravity flight experiment with a manned space vehicle. The experiment structural frame width is reduced to 500 mm so that the package can be installed and removed from a standard Space Lab rack. Utilizing the full 550 mm width would required modifying a standard rack, or mounting the experiment permanently in a standard rack both of which offer a potential weight savings by eliminating redundant structural members, but would complicate installation and ground test procedures. To facilitate the ground test phase of the program, the structure is free standing for floor or table mounting, thereby allowing complete access to all sides and the top of the package.

The individual experiment modules are packaged at a packing density that does not exceed the allowable 300 kg/m limit of the Space Lab racks. More dense packaging is possible if the allowable density is increased up to a maximum of 450 kg/m .

The experiment modules, and the control boxes are arranged within the structural framework to allow front (aisle side) access to those points requiring inflight man/experiment interfaces, and back or side access to all other experiments for servicing with the package removed from the equipment rack.

On the aisle side, access is available to the camera for film changing, to the processor for selection and startup of the experiment to be run, and to the control boxes for interchanging of electrical connectors to experiments Bu and Bw, and Du and Dw. Experiments A and F-1 are accessible from the aisle side during maintenance operations. Experiments Du, Dw, Bu, Bw, C, Eu, Ew, F-2a, F-2b, and F-2c are all accessible from the back side of the package. Experiments F-3a, F-3b, and F-3c are mounted together and are accessible from either side of the package. They are also accessible from the back of the package once experiments F-2a, b, and c have been removed. All package

HAMILTON STANDARD Division of UNITED TECHNOLOGIES

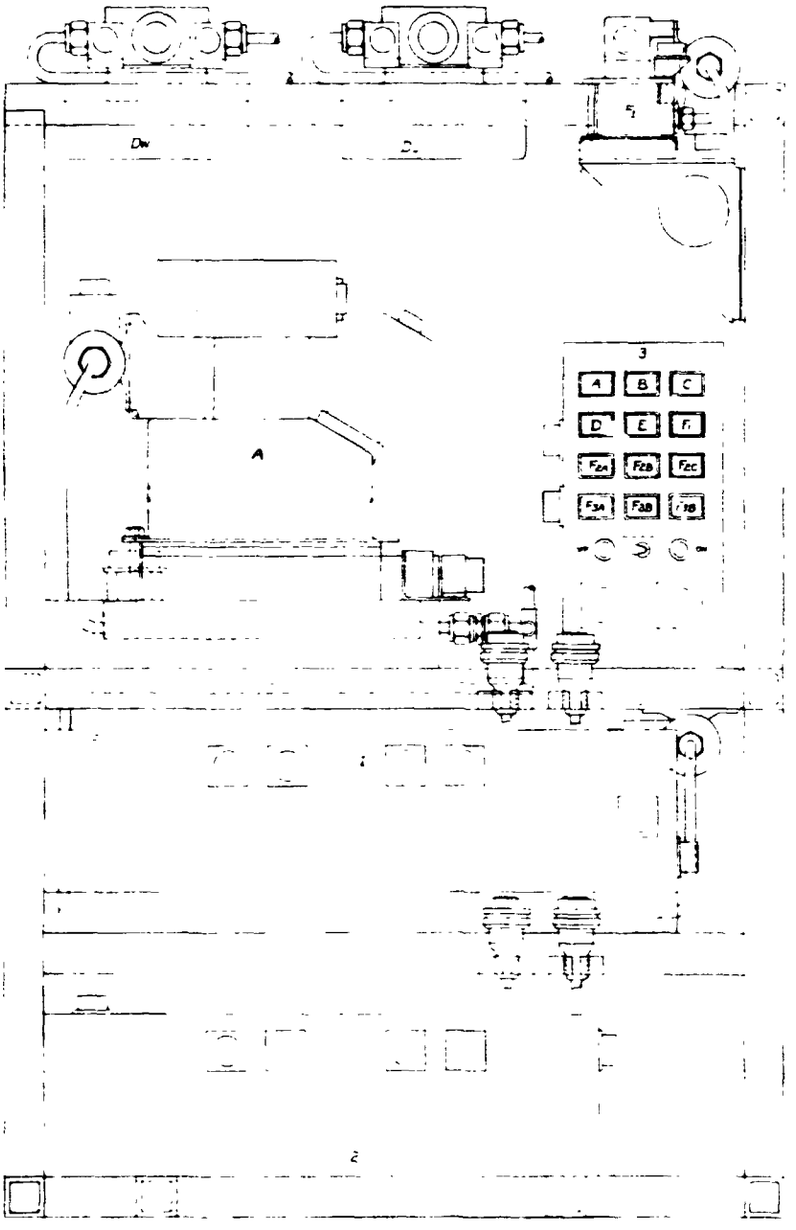

FRONT VIEW

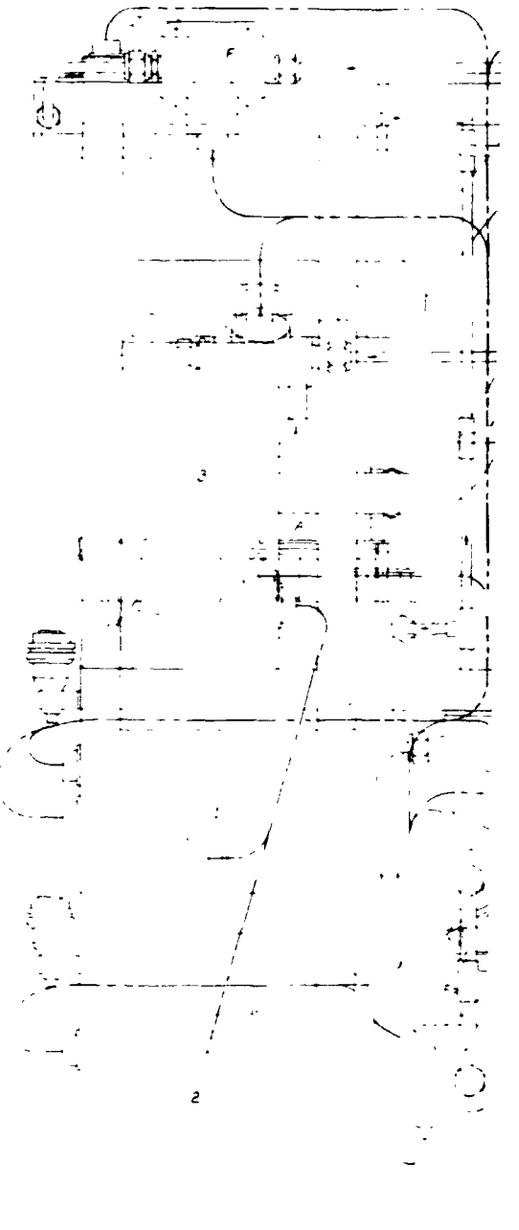

SIDE VIEW

FOLDOUT FRAME /

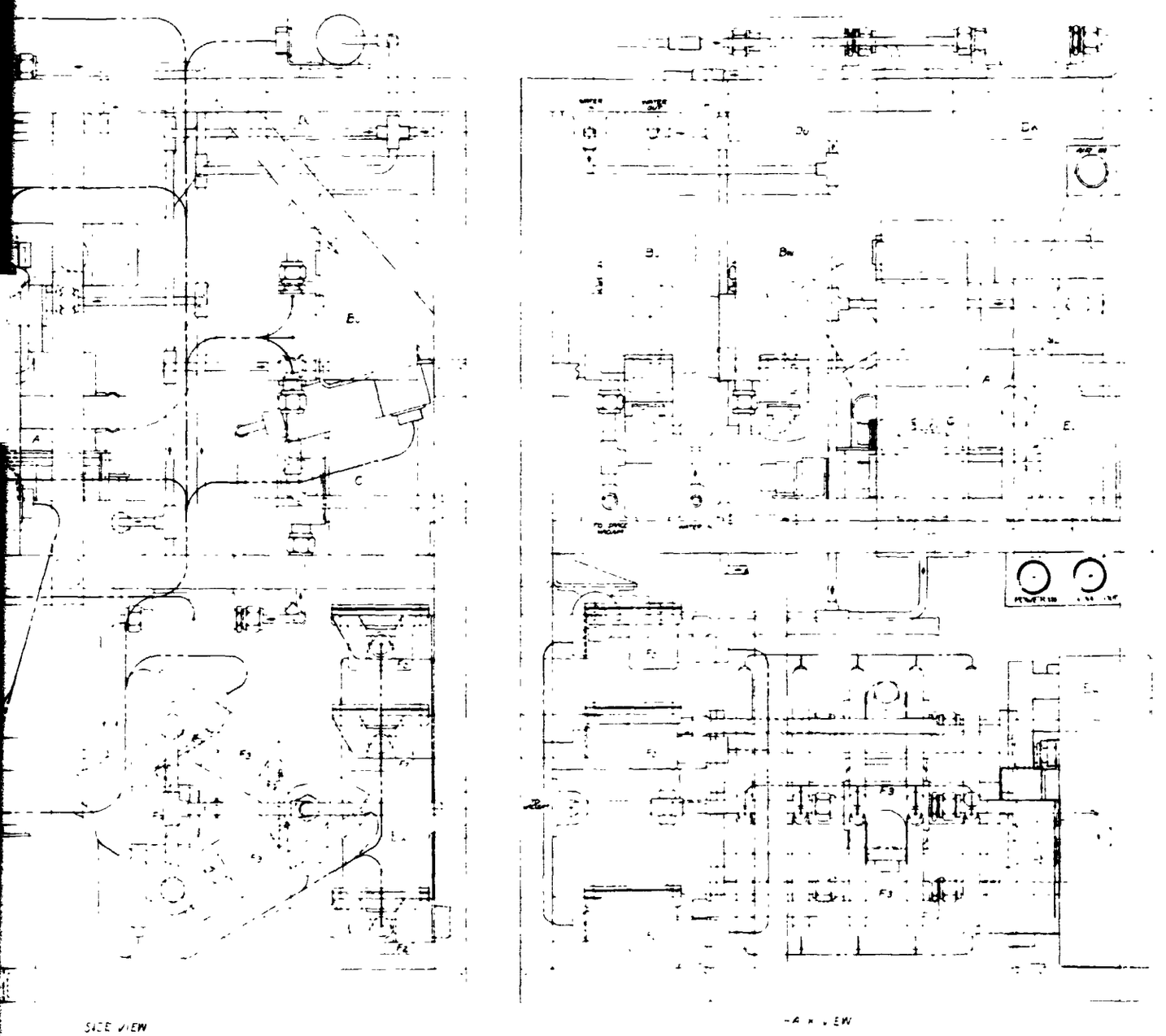

FIGURE 18:
PHYSICAL PHENOMENA EXPERIMENT CHEST PACKAGING ARRANGEMENT

FOLDOUT FRAME 2

interfaces, cooling water in and out, supply water in, space vacuum line, air in, electrical power in, and signals out are located on the back of the package where they connect to vehicle wiring and plumbing. The pipes and wires within the package are routed generally in the center of the package where they are supported at appropriate intervals by clamps and brackets, and where they do not interfere with individual experiment replacement. Each experiment is attached to the closest point of the package frame by mounting brackets. The frame and brackets are sized to handle the vibration and shock levels associated with a Shuttle Orbiter launch, bench handling, and shipping.

Weight, Volume, and Power Summary

Table IV shows a breakdown of the weights, volume , and power requirements of all the equipment in the Ice Pack Physical Phenomena experiment. The weights shown are maximum expected weights of the flight configuration as projected from the concept level of definition. The volume is representative of the overall envelope volume required for each experiment rather than a detailed "air displaced" volume. The power shown is indicative of the average power drain. Peaks for short duration switching and valve actuation, therefore, do not appear.

Experiment	Module Wet Weight kg	Number of Modules Required	Total Experiment Weight kg	Module Volume (Ref) in^3	Power While Running, Watts	
					115VAC	28VDC
A	5.38	1	5.38	0.01300	10	720
B	2.55	2	5.10	0.00265	6	-
C	3.15	1	3.15	0.00246	28	-
D	1.81	2	3.62	0.00236	90	-
E	3.32	2	6.64	0.00287	21	-
F1	2.00	1	2.00	0.00218	80	-
F2	0.46	3	1.38	0.00049	10	-
F3	1.76	3	5.28	0.01340	16	-
Processor	3.00	1	3.00	0.00262	22	-
Box 1	7.23	1	7.23	0.00737	30	60
Box 2	6.19	1	6.19	0.00642	2	10
Experiment Total			55.28			
Packaging			13.34			
Total Flight			68.62	.216		

Table IV Weight Power & Volume Summary

APPENDIX A

CITATIONS SELECTED FOR ACQUISITION AND REVIEW

1. Adler, M. J., Savkar, S. D., & Summerhayes, H. R., "Manipulation of Particles by Weak Forces", General Electric Co., Schenectady, N. Y., NASA-CR-120293.

2. Aladeu, I. T., & Ulianov, A. F., "Experimental Study of Heat Transfer During Boiling in Conduits During Weightlessness", Kosmicheske Issledovaniia (Cosmic Research), Vol. 6, Mar.-Apr. 1968.

3. Babskiy, V. G., Sklovskaya, I. L., and Sklovskiy, Y. B., "Thermocapillary Convection in Weightless Condition", Scientific Translation Service, Santa Barbara, California, 1973, NASA-TT-F-15535.

4. Bannister, T. C., Grodzka, P. G., Spradley, L. W., Bourgeois, S. V., Hedden, R. O., & Facemire, B. R., "Apollo 17 Heat Flow and Convection Experiments, Final Data Analyses Results", NASA, 1973.

5. Barton, J. E., & Patterson, H. W., "Apollo Oxygen Tank Stratification Analysis - Final Report", Boeing Company, Huntsville, Ala., 1972, D2118406-2.

6. Barton, J. E., & Patterson, H. W., "Post-Flight Analysis of the Apollo 15 Cryogenic Oxygen System", Boeing Company, Huntsville, Alabama, 1971, D2-1189422-1.

7. Belew, L. F. & Stuhlinger, E., "Skylab Guidebook", George C. Marshall Space Flight Center, Alabama, 1973.

8. Benard, H., "Les Tourbillous Cellulaires", Ann. Chem. Phys., Vol. 23, 1901.

9. Black, M. J., "Surface Tension as the Cause of Benard Cells and Surface Deformation in a Liquid Film", Nature, Vol. 178, 22 September 1956.

10. Bourgeois, S. V., "Convection Effects on Skylab Experiments M551, M552, M553", Lockheed Missiles and Space Company, Inc., Huntsville, Alabama, 1973, NASA CR-120482.

11. Bourgeois, S. V., "Physical Forces Influencing Skylab Experiments M551, M552, and M553", Lockheed Missiles and Space Company, Inc., Huntsville, Alabama, 1974, NASA CR-129037.

12. Bourgeois, S. V., & Brashears, M., "Fluid Dynamics and Kinematics of Sphere Forming Aboard Skylab II", paper given to AIAA 12th Aerospace Sciences Meeting, Washington, D. C., 30 January-1 February 1974.

13. Chambre, P. L., "On the Dynamics of Phase Growth", Quart. J. Mech. and Appl. Math., Vol. 9, 1956.

14. Chin, J. H., Donaldson, J. O., Gallagher, L. W., Harper, E. Y., Hurd, S. E., & Satterlee, H. M., "Analytical and Experimental Study of Liquid Orientation and Stratification in Standard and Reduced Gravity Field", Lockheed Missiles & Space Company, Palo Alto, Calif., July 1969, LMSC 2-05-64-1.

15. Cini, R., Loglio, G., & Ficalbi, A., "Anomalies in the Thermal Properties of Water", Istituto DI Chimica Fisica Dell Universite, Florence, 1969.

16. Clark, J. A., Lewis, E. W., & Merte, H., "Boiling of Liquid Nitrogen in Reduced Gravity", Michigan University, Ann Arbor, Michigan 1967, NASA-CR-98248.

17. Clement, J. R., & Gaffney, J., "Thermal Oscillation in Low-Temperature Apparatus", Adv. Cryogen. Eng., Vol. 1, 1954.

18. Cochran, T. H., "Forced Convection Boiling Near Inception in Zero Gravity", Lewis Research Center, NASA, Cleveland, Ohio, 1970, NASA TN-D-5612.

19. Conway, B. A., "Development of Skylab Experiment T-013 Crew/Vehicle Disturbance", 1972, NASA TN D6584.

20. Dodge, F. T., et. al., "Fluid Physics, Thermodynamics, and Heat Transfer Experiments in Space", Southwest Research Institute, San Antonio, Texas, 1974, NASA-CR-134742.

21. Doughty, J. O., & Henry, H. R., "Two Phase Flow and Heat Transfer in Porous Beds Under Variable Body Forces", University of Alabama, Huntsville, Alabama, 1969, NASA CR-108137.

22. Eckert, E.R.G., & Carlson, W. O., "Natural Convection in an Air Layer Enclosed Between Two Vertical Plates with Different Temperatures", Int. Heat Trans., Vol. 2, 1961.

23. Edeskuty, F. J., Williamson, K. D. & Taylor, J. F., "Pool Boiling Heat Transfer To Liquid Helium and Liquid Nitrogen In a Nearly Zero Gravity Environment", Los Alamos Scientific Lab, New Mexico, 1973, LA-UR-74-680.

24. Elder, J. W., "Laminar Free Convection in a Vertical Slot", J. Fluid Mech., Vol. 23, 1965.

25. Fan, C., "Convection Phenomena in Electrophoresis Separation", Lockheed Missiles & Space Company, Huntsville, Ala., 1972, LMSC-HREC TR D306300.

26. Fineblum, S. S., Haron, A. S., & Saxton, J. A., "Heat Transfer and Thermal Stratification in the Apollo 14 Cryogenic Oxygen Tanks", MSC Cryogenics Symposium Papers, 1971, MSC-04312.

27. Franke, B., & Peters, G., "Pamis Experiment Requirements", Erno Raumfahrttechnik GMBH, Bremen, 1973, ESRO CR(P)-455.

28. Glicksman, M. E., "Dynamic Effects Arising from High-Speed Solidification", Acta Metall., Vol. 13, 1965.

29. "Gravity - Sensitivity Assessment Criteria Study - Final Report", Convair Division of General Dynamics, San Diego, California, 1970, NASA CR 66945.

30. Grodzka, P. G., "Gravity Driven and Surface Tension Driven Convection in Single Crystal Growth", Lockheed Missiles and Space Co., Inc., Huntsville, Alabama, 1969, Marshall Space Flight Center Space Processing and Manufacturing Meeting, Oct. 21, 1969.

31. Grodzka, P. G., & Bannister, T. C., "Heat Flow and Convection Experiments Aboard Apollo 17", Lockheed Missiles and Space Company, Inc., Huntsville, Alabama, Science, Vol. 187, January 17, 1975.

32. Grodzka, P. G., & Bannister, T. C., "Natural Convection in Low G Environments", Lockheed Missiles & Space Company, Inc., Huntsville, Alabama, 1974, AIAA Paper No. 74-156.

33. Grodzka, P. G., & Bannister, T. C., "Heat Flow and Convection Demonstration Experiments Aboard Apollo 14", Lockheed Missiles and Space Company, Inc., Huntsville, Alabama, Science, Vol. 176, May 5, 1972.

34. Grodzka, P.G., & Bourgeois, S. V., "Fluid and Particle Dynamic Effects in Low-G", Lockheed Missiles &Space Company, Huntsville, Ala., 1973, LMSC-HREC TR D306402.

35. Grodzka, P. G., Bourgois, S. V., & Brashears, M. R., "Fluid Motions in a Low-G Environment", Lockheed Missiles and Space Company, Inc., Huntsville, Alabama, Proceeds of 3rd Space Processing Symposium on Skylab Results, Vol. 2.

36. Grodzka, P. G., Pan, C., & Hedden, R. O., "The Apollo 14 Heat Flow and Convection Demonstration Experiments; Final Results of Data Analysis", Lockheed Missiles & Space Company, Huntsville, Ala., 1971, LMSC-HREC D22533.

37. "Handbook of Chemistry and Physics", Chemical Rubber Publishing Co., Cleveland, Ohio, 1953.

38. Henderson, S. J., & Miller, R. I., "Study of Liquid-Solid Transition for Materials Processing in Space", Boeing Aerospace Company, Huntsville, Alabama, 1973, NASA-CR-124294.

39. Horvay, G., "Freezing into an Undercooled Melt Accompanied by Density Change", Proceed. U. S. National Congress of Appl. Mech., Vol. 2, Berkeley, Calif., 18-21 June.

40. Hung, R. J., Vaughan, O. H., & Smith, R. E., "A Zero-Gravity Demonstration of the Collision and Coalescence of Water Droplets", University of Alabama, Huntsville, Alabama, 1974.

41. Koschmieder, E. L., "On Convection Under an Air Surface", J. Fluid. Mech., Vol. 30, 1967.

42. Lacy, L. L. & Otto, G. H., "The Stability of Liquid Dispersions in Low Gravity", George C. Marshall Space Flight Center, Alabama, 1974, AIAA Paper No. 74-1242.

43. Larkin, B. K., "Heat Flow to a Confined Fluid in Zero Gravity", Progress in Astronautics and Aeronautics, Vol. 20, 1967.

44. Lienhard, J. H., "Gravity Boiling Studies", University of Kentucky, Lexington, Kentucky, 1971, NASA-CR-118638.

45. Linehard, J. M., & Dhir, V. K., "Extended Hydrodynamic Theory of Peak and Minimum Pool Boiling Heat Fluxes", Kentucky University, NASA-CR-2270.

46. Littles, J. W., & Merte, H., "Zero Gravity Incipient Boiling Heat Transfer", Space Transportation System Propulsion Technology Conference, Vol. 4, April 28, 1971.

47. "Marks Standard Handbook for Mechanical Engineers", McGraw-Hill, New York, 1967.

48. McGrew, J. L., "An Investigation of the Effect of Temperature Induced Surface Tension Gradients on Bubble Mechanics and Boiling Heat Transfer", Denver University, Colorado #68-13708, 1968.

49. Mehrabian, R., Keane. M., & Flemings, M. C., "Interdendritic Fluid Flow and Macrosegregation; Influence of Gravity", Met. Trans., Vol. 1, 1970.

50. Melcher, J. R., "Electrohydrodynamics", given at the IUTAM Moscow-Meeting, 1972.

51. Milly, N., & Gillespie, V. G., "Retention and Applications of Skylab Experiment Experiences to Future Programs", George C. Marshall Space Flight Center, NASA, Alabama, 1974, NASA TM X-64839.

52. Mossop, S. C., "The Freezing of Supercooled Water", Clarendon Laboratory, Oxford, England, 1954.

53. "MSFC Integrated Experiments Preliminary Report", George C. Marshall Space Flight Center, Alabama, 1974, NASA TM X-64881.

54. "MSFC Skylab Corollary Experiment Systems Mission Evaluation", George C. Marshall Space Flight Center, Alabama, 1974, NASA TM X-64820.

54A. "MSFC Skylab Mission Report - Saturn Workshop," George C. Marshall Space Flight Center, Alabama, 1974, NASA TM X-64814.

55. "MSFC Skylab Student Project Report", George C. Marshall Space Flight Center, NASA, Alabama, 1974, NASA TM X 64866.

56. Oker, E., & Merte, H., "Transient Boiling Heat Transfer in Saturated Liquid Nitrogen and F113 at Standard and Zero Gravity", University of Michigan, Ann Arbor, Michigan, 1973, NASA-CR-120202.

57. Ostrach, S., "Natural Convection in Enclosures", Advances in Heat Transfer, Vol. 8, Editors, J. P. Hartnett, and T. F. Irvine, Jr., Academic Press, New York, 1972.

58. Otto, G. H., & Lacy, L. L., "Observations of the Liquid/Solid Interface in Low-Gravity Melting", University of Alabama, Huntsville, Alabama, 1974, AIAA Paper No. 74-1243.

59. Pak, H. Y., Winter, E.R.F., & Schoenals, R. J., "Convection Heat Transfer in Contained Fluid Subjected to Vibration", Augmentation of Convective Heat and Mass Transfer, A. E. Bergles and A. L. Webb, eds., ASME, New York, 1970.

60. Palmer, H. J., and Berg, J. C., "Convective Instability in Liquid Pools Heated from Below", J. Fluid Mech., Vol. 47, 1971.

61. Pearson, J.R.A., "On Convection Cells Induced by Surface Tension", J. Fluid Mech., Vol. 4, 1958.

62. Povitskiv, A. S., & Ivubin, L. Y., "Certain Features of the Motion of a Fluid Under Weightlessness Conditions", International Astronautical Congress, Madrid, Spain, 1966, NASA TT F-10,868.

63. Prisnyakov, V. F., "Boiling Under Reduced Gravity Conditions", Kosmicheskie Issledovaniya, (Cosmic Research), Sept.-Oct. 1970.

64 "Proceedings - Third Space Processing Symposium - Skylab Results - Volume I", George C. Marshall Space Flight Center, Alabama, 1974, M-74-5-VI.

65. "Proceedings - Third Space Processing Symposium - Skylab Results - Volume II", George C. Marshall Space Flight Center, Alabama, 1974, M-74-5-V2.

66. Rayleigh, Lord, "On Convection Currents in a Horizontal Layer of Fluid When the Higher Temperature is on the Under Side", Phil. Mag., Vol. 32, (Ser. 6), 1916.

67. Rayleigh, Lord, "The Explanation of Certain Acoustical Phenomena", Nature, London, Vol. 18, 1878.

68. Rice, R. A., "Apollo 14 Flight Support and System Performance", MSC Cryogenic Symposium Papers, 1971, MSC-04312.

69. Saet, A. I., & Tatarchenha, V. A., "On the Relation Between Convective Instability in the Melt and the Stratified Distribution of Impurities During Crystallization", Bull. Acad. Sciences, USSR, Physical Series (Izvestiya Akademii Nauk SSSR, Seriya fizicheskaya), Vol. 36, 1972.

70. Scriven, L. E., & Sternling, C. V., "On Cellular Convection Driven by Surface - Tension Gradients", J. Fluid Mech., Vol. 19, 1964.

71. Shuttles, J. T., & Smith, G. L., "Stratification Calculations in a Heated Cryogenic Oxygen Storage Tank at Zero Gravity", MSC Cryogenics Symposium Papers, 1971, MSC-04321.

72. Siegel, R., "Effects of Reduced Gravity on Heat Transfer", Lewis Research Center, NASA, Cleveland, Ohio, 1967, Advances in Heat Transfer, Academic Press.

73. Smith, K. A., "On Convective Instability in Liquid Pools Heated from Below", J. Fluid Mech., Vol. 24, 1956.

74. Snyder, R. S., "Electrophoresis Demonstration on Apollo 16", 1972, NASA TM X-64724.

75. Spradley, L. W., "Thermoacoustic Convection of Fluids in Low Gravity", Lockheed Missiles & Space Company, Inc., Huntsville, Alabama, 1974, AIAA Paper No. 74-76.

76. "Study of Zero Gravity Capabilities of Life Support System Components and Processes", Convair Division of General Dynamics Corp., San Diego, Calif., 1968, NASA-CR-66534.

77. Symons, E. P., "Wicking of Liquids in Screens", Lewis Research Center, NASA, Cleveland, Ohio, 1974, NASA TN-D-7657.

78. Szekely, J., "Discussion of Convective Flow in Tin", Metall. Trans., Vol. 1, 1970.

79. Tobin, J. M., & Kossowsky, R., "Research Study on Materials Processing in Space", Westinghouse Electric Corporation, Pittsburgh, Pa., 1973, NASA CR-120479.

80. Ubbelohde, A. R., "Melting and Crystal Structure", Clarendon Press, Oxford, 1965.

81. Wexler, A., in Experimental Cryophysics, Edited by F. E. Hoare, et. al., Butterworths, London, 1961.

APPENDIX B

DERIVATION OF STEADY STATE HEAT TRANSFER EQUATION

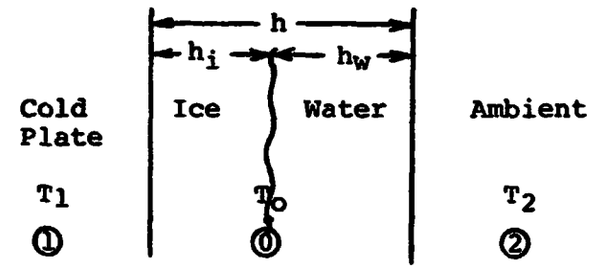

Sum Heat flow at Point ⓪

$$\dot{q}_{in} + \dot{q}_{out} = 0$$

$$\dot{q}_{in} = -\dot{q}_{out} = \bar{W} = \text{Heat Flux}$$

$$C_{ice}\,(T_1 - T_o) + C_w\,(T_2 - T_o) = 0$$

$$C_{ice} = \frac{K_1 A}{h_i}$$

$$C_w = \frac{K_2 A}{h_w}$$

$$\frac{K_1 A}{h_i}\,(T_1 - T_o) + \frac{K_2 A}{h_w}\,(T_2 - T_o) = 0$$

Since $T_o = 0^{\circ}C$

$$\frac{K_1 A}{h_i}\,T_1 = \frac{-K_2 A\,T_2}{h_w} = \bar{W}$$

or

$$\bar{W} = \frac{-K_2 A T_2}{h_w} \quad \text{EQUA. (A)}$$

$$A\left[\frac{K_1T_1}{h_i} + \frac{K_2T_2}{h_w}\right] = 0$$

$$h_i = h - h_w$$

$$A\left[\frac{K_1T_1}{h-h_w} + \frac{K_2T_2}{h_w}\right] = 0$$

$$A\left[\frac{K_1T_1h_w + K_2T_2(h-h_w)}{h_w(h-h_w)}\right] = 0$$

$$A\,(K_1T_1h_w + K_2T_2h - K_2T_2h_w) = 0$$

$$A\,(h_w\,[K_1T_1 - K_2T_2] + K_2T_2h) = 0$$

$$Ah_w\,[K_1T_1 - K_2T_2] + AK_2T_2h = 0$$

$$K_2T_2Ah = -\,Ah_w\,[K_1T_1 - K_2T_2]$$

$$\frac{K_2AT_2}{h_w} = \frac{-A}{h}\,[K_1T_1 - K_2T_2] \qquad \text{Equa. (B)}$$

Substituting Equa. (B) into Equa. (A)

$$\bar{W} = \frac{-AK_2T_2}{h_w} = \frac{A}{h}\,[K_1T_1 - K_2T_2]$$

Where A = heat transfer crossectional area = $\frac{\pi d^2}{4}$

$$\bar{W} = \frac{\pi d^2}{4h}\,[K_1T_1 - K_2T_2]$$